LA-7225-MS
Informal Report

UC-70
Issued: April 1978

# Stratigraphy of the Bandelier Tuff in the Pajarito Plateau.

## Applications to Waste Management

Bruce M. Crowe
George W. Linn
Grant Heiken
Mary Lou Bevier*

*Summer Graduate Student, University of British Columbia, Department of Geological Sciences, Vancouver, British Columbia, Canada V6T 1W5.

los alamos
scientific laboratory
of the University of California
LOS ALAMOS, NEW MEXICO 87545

An Affirmative Action/Equal Opportunity Employer



UNITED STATES
DEPARTMENT OF ENERGY
CONTRACT W-7405-ENG. 36

# STRATIGRAPHY OF THE BANDELIER TUFF IN THE PAJARITO PLATEAU. APPLICATIONS TO WASTE MANAGEMENT

by

Bruce M. Crowe, George W. Linn, Grant Heiken, and Mary Lou Bevier

## ABSTRACT

The Bandelier Tuff within the Pajarito Plateau consists of a lower sequence of air-fall and ash-flow deposits (Otowi Member) disconformably overlain by an upper sequence of air-fall and ash-flow deposits (Tshirege Member). The ash-flow sequence of the Tshirege Member consists of three cooling units throughout much of the Pajarito Plateau. The lower cooling unit is formed by three to as many as six pyroclastic flow units; the middle and upper cooling units each consist of at least three pyroclastic flow units. The contact between the lower and middle cooling unit coincides with a pyroclastic flow unit contact. This horizon is a prominent stratigraphic marker within distal sections of the Tshirege Member.

Major and trace element analyses of unaltered and altered samples of the Bandelier Tuff were determined by neutron activation and delayed neutron activation techniques. Petrographic, granulometric and morphologic characteristics of the Bandelier Tuff were determined to provide background information on the suitability of the Tuff as a medium for radioactive waste disposal.

The hydrologic characteristics of the Bandelier Tuff are controlled primarily by secondary features of the Tuff (cooling zones). These features vary with emplacement temperature and transport distance of the Tuff. Primary depositional features provide second order control on transport pathways in distal sections of the Tuff.

---

## I. INTRODUCTION

The Jemez Mountains, located in north-central New Mexico, are composed in major part of a thick accumulation of volcanic and volcaniclastic rocks ranging in age from Pliocene to recent (Ross and others, 1961; Doell and others, 1968).

Eruptive activity from this complex volcanic center culminated with the outpouring of the Bandelier Tuff, a large volume (>400 $km^3$ uncorrected for density) sequence of ash-flow and air-fall deposits. The deposits of the Bandelier Tuff form broad plateaulands that nearly encircle the Jemez Mountains and dip gently away from the Valles Caldera. The plateau on the east side of the Jemez Mountains, referred to as the Pajarito Plateau, consists of a series of east to southeast-trending, finger-like mesas that are separated by deeply incised canyons. The Los Alamos Scientific Laboratory is located on the Pajarito Plateau, between Frijoles and Pueblo Canyons.

Since the 1940's, radioactive wastes have been buried on Laboratory property (Wheeler and others, 1977). The rock medium for waste burial is the Bandelier Tuff, in major part, the Tshirege Member of the Tuff. In early 1977, geologic and geochemical characterization of the Bandelier Tuff was undertaken as part of a program evaluating the geology of the waste disposal sites. The purposes of these studies were twofold:

(1) To determine the detailed stratigraphy of the Bandelier Tuff in the Pajarito Plateau. Based on these determinations, which proceeded from the foundation of previous stratigraphic studies (Ross and others, 1961; Griggs, 1964; Smith and Bailey, 1966; Bailey and others, 1969), physical and structural characteristics of the Tuff are identified that may control transport pathways during possible migration of radioactive waste.

(2) To determine the geochemical environment of the Bandelier Tuff and identify mass transfer of elements by natural alteration processes affecting the Tuff.

This report is presented to summarize the results of stratigraphic, geochemical, and petrographic studies of the Tuff with applications to waste management. The geochemical and petrographic studies are still in progress and only preliminary results are reported. Several major reports describing the detailed volcanic geology of the Jemez Mountains are currently in preparation by R. L. Smith and R. Bailey of the U.S. Geological Survey (R. Bailey, personal communication, 1977). We have directed this study toward upgrading current stratigraphic data for the Tuff in the vicinity of Laboratory property using field techniques required to evaluate the geology of the complex ash-flow sheet.

Such information will provide valuable background stratigraphic data for future studies of the Tuff in the newly established National Environmental Research Park.

## II. PREVIOUS WORK

The term "Bandelier Tuff" was first used by H. T. U. Smith (1938). Griggs (1964) formally incorporated the Bandelier Tuff as a stratigraphic unit and included the rocks within the Tewa Group. He divided the Tuff into three Members that include, from bottom to top: the Guaje Member, the Otowi Member, and the Tshirege Member. Bailey and others (1969) renamed the Guaje Member the Guaje Pumice Bed and included it within the Otowi Member. They formally defined the Tsankawi Pumice Bed and included this sequence of air-fall deposits within the Tshirege Member. The stratigraphic classification of Bailey and others (1969), which is based on recognition of major eruptive cycles within the Bandelier Tuff, is preferred in this report.

The first comprehensive summary of the geology of the Jemez Mountains was by Ross and others (1961). They recognized that the Bandelier Tuff could be divided into two distinct, and petrologically related eruptive sequences: a basal sequence of air-fall (Plinian deposits, Walker, 1973) and overlying ash-flow deposits (Otowi Member) overlain disconformably by a second sequence of air-fall and ash-flow deposits (Tshirege Member). Griggs (1964) described the stratigraphy and hydrology of the Los Alamos area and included a map of the Pajarito Plateau (scale 1:24,000).

Smith and Bailey (1966) published a summary account of the geology of the Tshirege Member of the Bandelier Tuff including the distribution, stratigraphy and preliminary mineralogy and chemistry. The important conclusions of their work are summarized below (from Smith and Bailey, 1966):

(1) The Bandelier Tuff represents two cycles of ash-flow eruption and caldera formation -- the climactic phase of a long history of volcanism in the Jemez Mountains.

(2) The Tshirege Member of the Bandelier Tuff was divided into five subunits. The subunits are composed of groups of ash flows or stratigraphic zones that can be correlated over the entire outcrop area of the Bandelier Tuff. These subunits were determined from numerous stratigraphic sections and multiple physical and structural

features. The subunits are identifiable primarily on the basis of those characteristics that reflect relative emplacement temperature (welding and crystallization) and mineralogy.

(3) The ash-flow sequence of the Tshirege Member (basal 60%) records a systematic increase in emplacement temperature.

(4) Mineralogical variations within the Tshirege Member include a slight trend toward more sodic alkali feldspar upward in section (from the air-fall base up through subunits I-IV), the occurrence of zoned anorthoclase in subunit IV, restriction of fayalite to sanidine-bearing pumice and an increase in total modal phenocryst content from 5% in the air-fall deposits to 35% near the top of unit III followed by a mark decrease to 20% (the decrease in phenocryst content coincides with the onset of preferential resorption of quartz).

(5) Bulk chemical compositions of the Tshirege Member show major and trace element trends indicating the material erupted first was most salic and the last erupted most mafic. These trends are consistent with the interpretation that the Tuff was erupted from the upper part of a compositionally zoned magma chamber.

Smith and Bailey (1968) defined and described the stages of development of resurgent cauldrons. The volcanic cycles of the Valles Caldera, including the eruption and emplacement of the Bandelier Tuff, were used as a model of the seven stages of development in the evolution of a resurgent cauldron. Doell and others (1968) presented the results of paleomagnetic and potassium-argon studies of volcanic rocks associated with the Valles Caldera. The Otowi Member of the Bandelier Tuff was dated at about 1.4 Myr; the Tshirege at about 1.1 Myr. Sommer (1977) examined the composition of melt inclusions in quartz phenocrysts from air-fall and ash-flow deposits of the Tshirege Member. He inferred volatile contents as great as 7 wt% and averaging 5 wt% for samples of Tsankawi air-fall pumice. Eichelberger and Koch (1978) have completed a study of the occurrence and distribution of lithic fragments in the Bandelier Tuff.

## III. NOMENCLATURE

Ash-flow tuff or ignimbrite, the more common term in international usage, forms the majority of the Bandelier Tuff. These rocks were emplaced at variable temperatures (<100°C to as great as 800° or 900°C; Smith and Bailey, 1966) as

fluidized, particulate density flows or ash flows. The major features of ash flows and ash-flow deposits (ignimbrites) have been reviewed by Smith (1960a, 1960b) and Ross and Smith (1961).

The fundamental unit in stratigraphic and field studies of ignimbrites is the cooling unit. A cooling unit consists of the deposits of an ash flow or sequence of ash flows that cooled as a single unit (Smith, 1960a). A simple cooling unit exhibits characteristic welding and compaction zones (Smith, 1960b, Riehle, 1973). A compound cooling unit is one that departs from the expected zonations that should result from an uninterrupted cooling history. The recognition and identification of these zones, which are shown on Fig. 1, are a basic field procedure in determining cooling units within a complex ash-flow field.

Superimposed on welding and compaction zones of simple and compound cooling units are:

- Zones of devitrification.
- Zones of vapor-phase crystallization.
- Zones of fumarolic alteration.

Additionally, there is a progressive temperature loss during eruption, transport, and emplacement of ignimbrites. Consequently ignimbrites deposited on the distal edges of an ash-flow field will differ in physical characteristics from proximal deposits. Commonly there will be cooling breaks in the distal parts of ash-flow fields that are not recognizable toward the source. In this manner, single cooling units in the proximal parts of an ash-flow field can be traced laterally into compound cooling units (Smith, 1960b; see also Smith and Bailey, 1966, their Fig. 8).

Sparks and others (1973) established criteria for the recognition of flow units in ignimbrites. Their work, which evolved from years of study of ignimbrites (Taylor, 1958; Smith, 1960a; Fisher, 1965; Walker, 1971), provides the basis for determining the depositional history and reconstructing eruptive events in a major ash-flow field.

In the ideal case, deposits formed by the passage of a single ash flow exhibit a characteristic textural zonation shown in Fig. 2. Basal deposits of a single flow unit generally consist of lenticular, moderately well-sorted, laminated, and locally cross-bedded, crystal-rich tuff referred to as pyroclastic surge deposits (Sparks, 1976). These rocks are probably emplaced from a dilute (low-particle concentration) density flow analogous to the base surge of

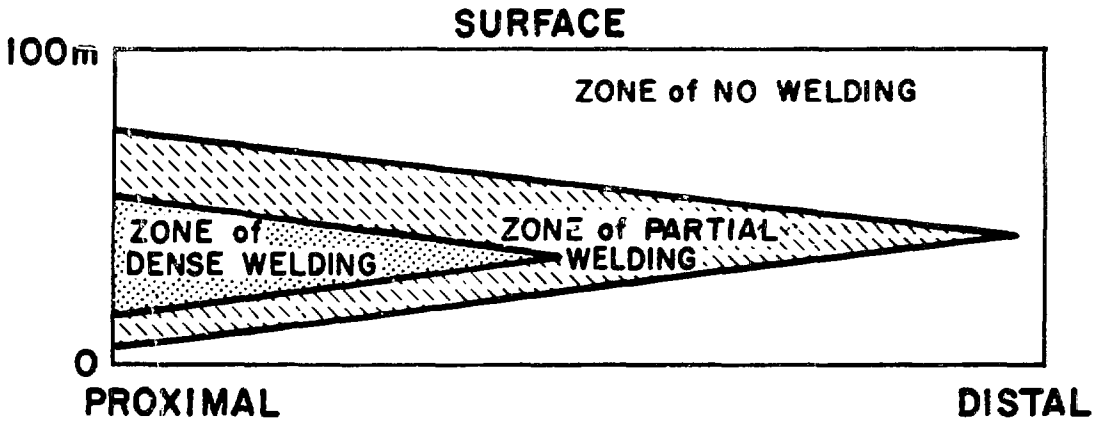


Fig. 1.

Generalized configuration of welding zones in a simple cooling unit. Note thinning and pinch-out of welding zones with increased lateral distance from source. Modified from Smith (1960b).

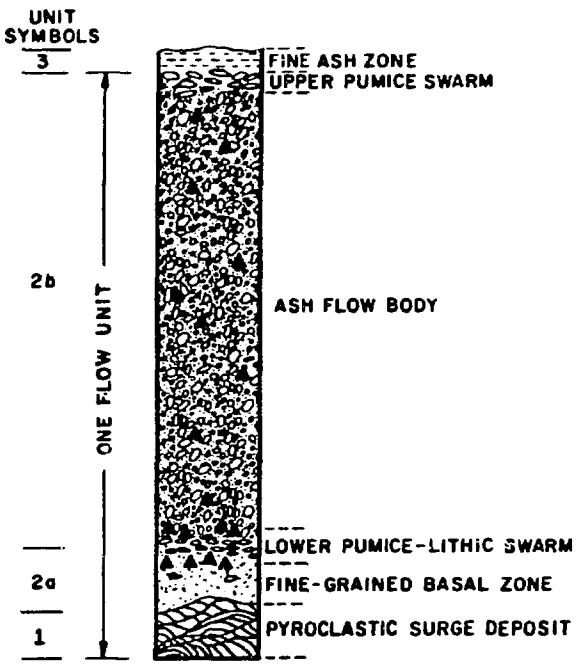


Fig. 2.

Textural zones produced by the passage and deposition of a single flow unit or ash-flow. Unit symbols after Sparks and others (1973). Due to intertonguing of pyroclastic surge deposits and deposits of the fine-grained basal zone in flow units of the Bandelier Tuff, we have extended the flow unit to include the pyroclastic surge deposits (contrast with Sparks and others 1973, Fig. 1).

phreatomagmatic eruptions (Fisher and Waters, 1969; Crowe and Fisher, 1973). Pyroclastic surge deposits are overlain by ash-flow deposits that can be divided into two zones: a fine-grained basal tuff characterized by an absence or low abundance of pumice and lithic fragments (fine-grained basal layer of Fig. 2) and overlying poorly sorted tuff with a fabric and grain-size characteristics typical of well-described ash-flow deposits (ash-flow body of Fig. 2). The gradational contact between these zones is generally marked by an increase in abundance of lithic and pumice fragments (lower pumice-lithic swarm of Fig. 2). The top of the ash-flow body is commonly characterized by a second zone of increased pumice concentration (upper pumice swarm). Finally, overlying the ignimbrite are fine-grained, vitric ash probably deposited by aerial fallout from the ash cloud associated with emplacement of an ash flow. These deposits are rarely preserved in the geologic record (Sparks and others, 1973).

Our studies of the physical stratigraphy of the Bandelier Tuff are concerned with the recognition and description of natural rock properties that may control transport paths within the Tuff. Accordingly, we have identified two classes of rock features: primary depositional features and secondary features. Primary depositional features are those structures that are formed during transport and deposition of pyroclastic fragments. They include, for example, the major textural zones of a flow unit. Secondary features include those structures formed after deposition of the Tuff. Examples include welding zones, cooling joints, and others (primarily cooling features).

## IV. STRATIGRAPHY OF THE BANDELIER TUFF

Stratigraphic sections in the Bandelier Tuff were measured in three major areas of the Pajarito Plateau (Fig. 3). For each area, data were combined from the sections to construct composite columns. All sections were measured by tape and brunton and primary and secondary features of the tuff were noted. Composite stratigraphic columns were constructed for several reasons

- They illustrate the stratigraphy of the Tuff for a relatively large area. Because of the lateral variability of the Tuff, single measured sections provide detailed stratigraphic data for only that site. Composite columns extend the lateral applicability of stratigraphic data.

- By examining and combining numerous stratigraphic sections, we have observed and recorded many physical features that are not recognizable at any single locality.

The major areas represented by the composite columns were carefully chosen. Columns one and three were constructed from distal areas of the ash-flow sheet (Fig. 3). Here welding effects are minimal and primary depositional features can be determined in detail. Column two was constructed from more proximal areas of the ash-flow sheet where secondary features are well developed.

A. Composite Column One

Within the section area of composite column one (Fig. 3), the Bandelier Tuff rests unconformably on the Puye Formation and locally overlies lava flows of the basalt of Cerros del Rio (Fig. 4). This section area is significant for two reasons. First, it is one of only several areas within the Pajarito Plateau where extensive deposits of the Otowi Member are both preserved and exposed (see Smith and others, 1970) and second, here the Bandelier Tuff is unusually thick (average thickness approximately 100 m). The thickened sections of the Tuff and presence of the Otowi Member are probably due to emplacement within the Puye depositional basin (see Smith and others, 1970).

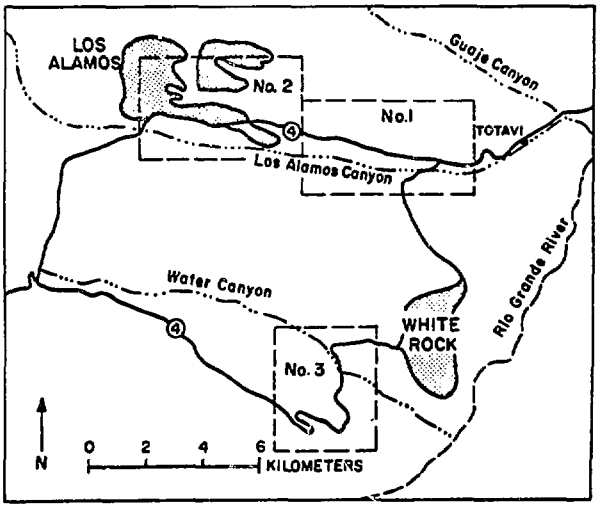


Fig. 3.
Location map of areal zones for composite columns one, two, and three.

1. Otowi Member

The Otowi Member consists of the basal Guaje Pumice bed and overlying ash-flow deposits (Bailey and others, 1969).

a. Guaje Pumice Bed

The Guaje Pumice Bed is exposed only in Los Alamos Canyon, several kilometers west of Totavi (Fig. 5). It locally rests on the basalt of Cerros del Rio. However, at most exposures, the deposits overlie lenses of tuffaceous siltstone (0-1 m thick) deposited in topographic lows on the basalt surface. The Guaje Pumice Bed consists of silicic air-fall deposits (Griggs, 1964). The deposits are

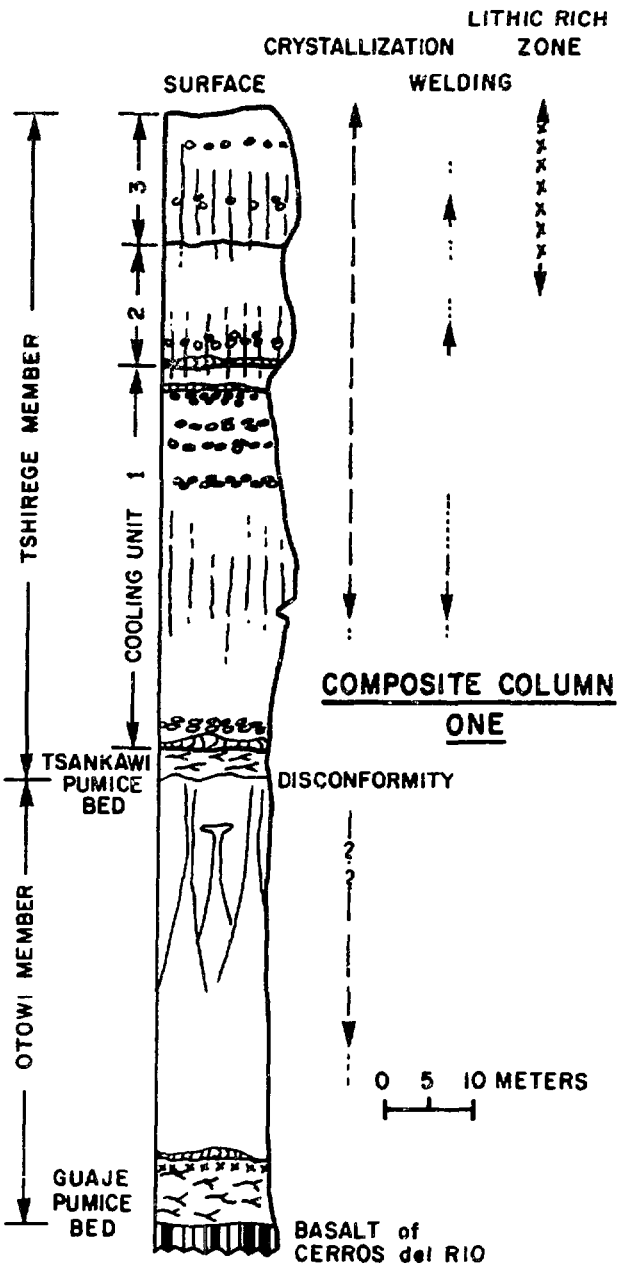


Fig. 4.

Primary depositional features and secondary features of the Bandelier Tuff, composite column one. Symbols represent, from bottom to top of column: (1) Y-shaped shards - air-fall pumice deposits (Plinian deposits); (2) x's - horizon of marked enrichment in abundance of lithic fragments; (3) lenticular, cross-hatched zones - pyroclastic surge deposits; (4) unfilled elipses - pumice swarms; (5) funnel-shaped pipes - fumarolic pipes; (6) vertical lines - zones of columnar jointing. Crystallization refers to vapor-phase crystallization.

Fig. 5.

Outcrop of Guaje Pumice Bed along Highway 4 several kilometers west of Totavi. The Guaje Pumice Bed rests on basalt and tuffaceous siltstone. Note absence of bedding except in the upper part of the sequence.

massive to poorly bedded with bedding surfaces mantling underlying topographic irregularities. The Guaje Pumice Bed consists of unconsolidated, lapilli-tuff formed primarily of subangular to angular pumice averaging 2 to 4 cm in size (range 3 mm to 6.5 cm). Development of bedding in the Guaje Pumice Bed increases upward in section due primarily to a decrease in abundance of coarse pumice fragments (increase $\sigma$). The upper 0.2 m of the Guaje Pumice Bed, directly underlying ash-flow deposits, consist of lenticular-bedded tuff with subrounded pumice fragments and crystal-rich lenses. These air-fall deposits are probably wind reworked. This reworking may be due to two possible mechanisms: local winds reworking the depositional interface during a pause in eruptive activity and/or reworking by the air blast that preceded emplacement of the overlying ash flow.

The Guaje Pumice Bed is relatively crystal and lithic poor. There is an slight increase in the volume percent of crystal and lithic fragments upward in section. Approximately 1 m below the top of the deposit, there is a horizon of marked coarsening of the pumice fragments (1-5 cm) and increase in the size (1-3 cm) and abundance of lithic fragments. An upward increase and distinct horizons of enrichment in lithic fragments in large Plinian deposits may be attributed to eruptive vent widening and fragment engulfment (Wilson, 1976; R. S. J. Sparks, personal communication, 1977).

b. Ash-Flow Deposits

The Guaje Pumice Bed is overlain by a thick sequence of ash-flow deposits that form most of the Otowi Member (Fig. 4). Basal tuff of the ash-flow sequence comprises lenticular pyroclastic surge deposits (3 cm to 0.5 m thick) that grade upward into lithic and pumice-poor tuff corresponding to the fine-grained basal layer of a pyroclastic flow unit (Fig. 2). These in turn are overlain by one to several horizons of pumice swarms that grade upward into typical ash-flow deposits (zone 2b of Sparks and others, 1973). Thus the basal part of the ash-flow sequence of the Otowi Member exhibits a pyroclastic flow unit zonation.

The ash-flow sequence of the Otowi Member consists of poorly sorted, tuff to lapilli-tuff. In contrast to the underlying air-fall sequence, the deposits are massive to poorly bedded. Bedding, where present, is defined by parallel elongation or imbrication of pumice fragments. Pumice fragments are subrounded to rounded and individual fragments are supported in an ash matrix. Median diameter ($Md_\phi$) versus Inman sorting coefficient ($\sigma_I$) of samples from the ash-flow sequence are plotted on a graph showing Walker's (1971) empirically derived airfall and pyroclastic flow fields (Fig. 18). The samples plot within the flow field.

In most areas, flow unit contacts were not recognized within the ash-flow sequence above the basal zones. However, in a minor tributary canyon to Pueblo Canyon, a prominent flow-unit contact with well-developed flow unit textural zones (Fig. 6) can be traced laterally for 1 km. Thus within the area of composite column one, the ash-flow sequence of the Otowi Member appears to consist of two flow units.

The ash-flow sequence of the Otowi Member is unwelded in all exposures in the Pajarito Plateau. In marked contrast, the sequence is locally densely welded on the west side of the Jemez Mountains. Vapor-phase crystallization,

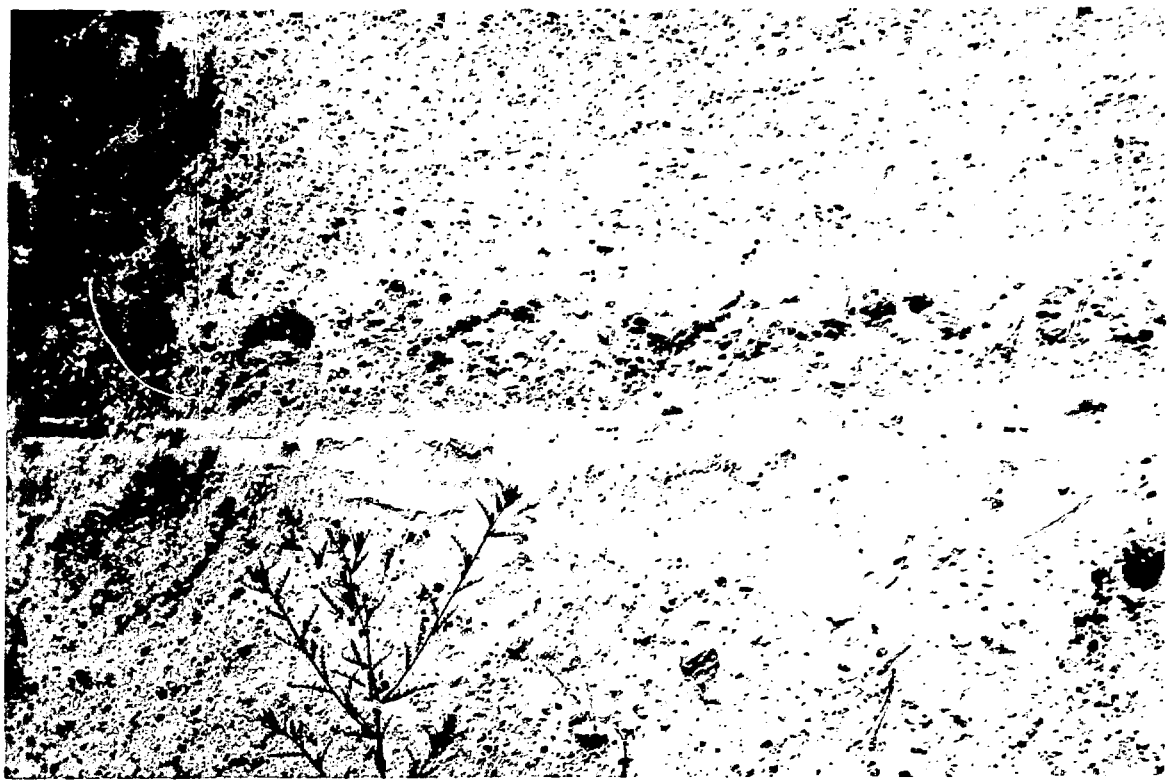

Fig. 6.

Flow-unit contact within the ash-flow sequence of the Otowi Member. Note very thin fine-grained basal layer directly underlying well-developed pumice swarm in the lower part of the upper flow unit. Pyroclastic surge deposits (1 to 3 cm thick) underlie the fine-grained basal layer and the base of the surge deposits is the contact between the two flow units.

noted by the appearance of cristobalite and tridymite in pumice clasts, occurs approximately 8 m above the base of the ash-flow sequence and extends to near the top of the section (Fig. 4). Well-developed fossil fumarolic pipes are present at several localities; notably in road cuts several kilometers west of Totavi and in lower Pueblo Canyon (Fig. 7).

The upper contact of the Otowi Member is an erosional surface marked by a horizon, 0.2 to 1 m thick, of epiclastic deposits and partial soil development. Reworked deposits include epiclastic and tuffaceous siltstone to sandstone with conglomeratic lenses containing large pumice fragments (up to 1 m) reworked from

Fig. 7.

Well-developed fossil fumarole pipes within the ash-flow sequence of the Otowi Member. The resistant cap rock of individual pipes is a horizon of increased fumarolic mineralization.

the Otowi Member and volcanic clasts eroded from the Jemez volcanic highland. The partial soil zone is a horizon of oxidization and clay development cross-cut by irregular fractures infilled with secondary alteration material.

K-Ar ages of the Otowi Member (1.09 Myr) and the Tshirege Member (1.37 Myr) were determined by Doell and others (1968). Based on statistical analyses of these data, they established a maximum confidence, P, of >99% that the difference between the ages are real. The exact duration of the hiatus between the members is unknown, but clearly the erosional interval is a reflection of this time gap.

2. Tshirege Member

The Tshirege Member of the Bandelier Tuff rests unconformably (disconformity) on the Otowi Member. The former Member, like the latter, is divided into two eruptive sequences; a sequence of Plinian fall deposits (Tsankawi Pumice Bed) and an overlying sequence of petrologically related ash-flow deposits (Smith and Bailey, 1966).

a. Tsankawi Pumice Bed

Within the area of composite column one, the Tsankawi Pumice Bed is exposed discontinuously in the cliff walls of Los Alamos, Pueblo, Bayo, and Sandia Canyons. The thickness of the deposits is variable due to differences in the amount of reworked (tuffaceous and epiclastic) debris present in the section. The Tsankawi Pumice Bed consists of tuff to lapilli-tuff, air-fall deposits. The unit can be divided into three to five sequences separated by reworked deposits. The most coarse deposits are the basal pumice fall (0.4 to 1 m thick); maximum pumice size exceeds 5 cm. Succeeding air-fall deposits are of variable, but generally finer grain size. Two of the sequences contain abundant perlitic lithic fragments and accretionary lapilli. Locally the Tsankawi contains distinctive gray pumice with abundant crystals of accicular hornblende (Bailey and others, 1969).

b. Ash-flow Deposits

Ash-flow deposits of the Tshirege Member overlie the Tsankawi Pumice Bed. These deposits are complex and laterally variable. They form a multiple flow, composite ash-flow sheet (Smith, 1960a, Smith and Bailey, 1966; Doell and others, 1968). The deposits compose the major part of canyon cliffs on the Pajarito Plateau and are the principal unit in which radioactive waste material has been, and is currently emplaced (Wheeler and others, 1977). For continuity of discussion, the secondary features of the ash-flow deposits are described first, followed by primary depositional features.

(i) Secondary Features. In the area of composite column one, the ash-flow sequence is divided into three cooling units (Fig. 4). The uppermost cooling unit is only locally present and where present, is significantly eroded. The major features of the cooling units are illustrated in Fig. 4.

Cooling unit one is the thickest cooling unit of composite column one. The pyroclastic deposits of the cooling unit were emplaced over an irregular erosional surface and consequently thicken in topographic lows and thin over

topographic highs. Deposits of the basal one-third of the unit are unwelded. The onset of welding is marked by induration of the tuff and visible pumice compaction. The welding zone of cooling unit one is a cliff forming zone and coincides in section with the development of columnar cooling joints. Because of the degree of induration from welding and compaction and the jointing, the zone of partial welding within cooling unit one forms a distinctive horizon (Fig. 8; see also Smith, 1960a, Plate 1). The uppermost part of cooling unit one is unwelded and is a slope forming unit (Fig. 8). Cooling unit two is approximately 15 m thick (average thickness). It has a thin, approximately 1 m

Fig. 8.

Cliff exposures of the Bandelier Tuff, northern Bayo Canyon. Talus covered, slope-forming unit in the lower part of the photograph is the ash-flow sequence of the Otowi Member. The Tsankawi Pumice Bed is not exposed. The cliff section is formed by the ash-flow sequence of the Tshirege Member. The ash-flow sequence here consists of three cooling units. Prominent ledge in the lower part of the ash-flow sequence is the erosional notch marking the onset of abundant vapor-phase crystallization.

thick unwelded base, overlain by a 5-m zone of partial welding in turn overlain by unwelded deposits. Cooling joints in cooling unit two coincide with the zone of partial welding and extend down section through the unwelded base and into the upper part of cooling unit one. Cooling unit three is only partly preserved and exhibits welding and compaction zonation similar to cooling unit two (Fig. 4).

Vapor-phase crystallization in the ash-flow sheet controls the weathering and color properties of part of the sequence. The onset of vapor-phase crystallization in the Tuff coincides with a horizon of orange colored tuff, probably due to oxidation of femic constituents. Approximately 1 m above the first appearance of vapor-phase crystallization within cooling unit one is a thin (1-m) horizon that preferentially erodes to form a prominent ledge. This ledge is a distinctive feature of the Bandelier Tuff throughout the Pajarito Plateau (Fig. 8). The origin of the easily eroded zone is complex. It occurs within the lower part of the welded zone of cooling unit one several meters above the horizon marked by the onset of incipient welding and below the zone of recognizable pumice compaction. It is a horizon marking the onset of abundant vapor-phase crystallization. The preferential erodability of this zone is attributed to a complex interrelationship between vapor-phase crystallization and degree of welding. Below the soft zone the Tuff is incipiently welded resulting in increased induration [(a) of Fig. 9]. Within the soft zone (b), vapor-phase crystallization overshadows induration from welding resulting in a crumbly, unconsolidated rock. Above (b) as welding intensity increases and overshadows the effects of vapor-phase crystallization, the Tuff is resistant to erosion. These considerations are shown graphically in Fig. 9. Smith (1960a, p. 828) has noted that coarse vapor-phase crystallization will render a mildly welded tuff less coherent. Sheridan (1970) noted that in the upper part of the Bishop Tuff, a break in slope above cliff-forming densely welded tuff coincides with the superposition of vapor-phase crystallization on devitrification. A preferentially eroded notch coinciding with the onset of coarse vapor-phase crystallization within incipiently welded tuff has been observed in the Thirsty Canyon Tuff of the Nevada Test Site (B. Crowe, unpublished field notes, 1977).

(ii) Primary Depositional Features. Basal deposits of the ash-flow sequence of the Tshirege Member overlie the Tsankawi Pumice Bed. These deposits form the lower part of a flow unit. Pyroclastic surge deposits overlie and locally have eroded the upper part of the Tsankawi Pumice Bed. The surge

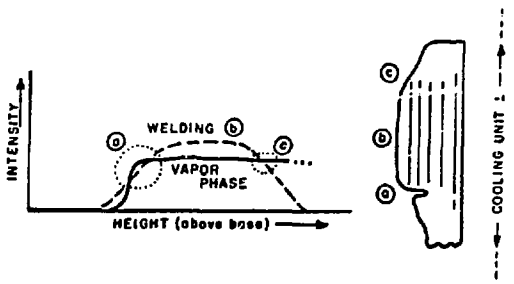


Fig. 9.
Schematic illustration of coincidence of erosional notch with onset of abundant vapor-phase crystallization in cooling unit one. Intensity represents dimensionless measure of degree of welding and abundance of vapor-phase crystallization. See text discussion.

deposits grade upward into fine-grained tuff (fine-grained basal layer) that in turn grade upward into one to several pumice swarms. The pumice swarms are overlain by ash-flow deposits that constitute the flow-unit interior (ash-flow body).

Above the basal zone, primary depositional features are present in the upper part of cooling unit one above the zone of partial welding (Fig. 4). Here three to five distinct pumice swarms, each with a fine-grained basal zone (Fig. 10), probably represent thin flow units. They are similar to thin flow units described by Sparks (1975) in the ignimbrites of Vulsini Volcano, central Italy. The lowermost pumice swarm is not underlain by a recognizable fine-grained basal layer; rather it is overlain, the contact being an erosional surface, by fine-grained tuff. This suggests that the pumice swarm is a flow-unit top. Accordingly the lower 25 m of cooling unit one may have been emplaced as a single, thick cooling unit.

The contact between cooling unit one and cooling unit two is an important contact. It separates two distinct cooling units and thus represents an eruptive hiatus of limited but nontheless significant duration. The contact is marked by well-developed flow unit textural zones, the features of which are shown in Fig. 11. It is a type example of a flow-unit boundary coinciding with both a cooling and eruptive break. Additionally, the contact is a prominent stratigraphic marker within distal parts of the Tshirege Member throughout the Pajarito Plateau.

Unwelded upper deposits of cooling unit two grade upward into unwelded deposits of cooling unit three without evidence of a flow unit contact. However, thin discontinuous and poorly developed pumice swarms are present in cooling unit three and may represent incipient stages in the development of a flow unit.

The upper unwelded zone of cooling unit two and cooling unit three are formed by ash-flow deposits containing a marked increase in the abundance and

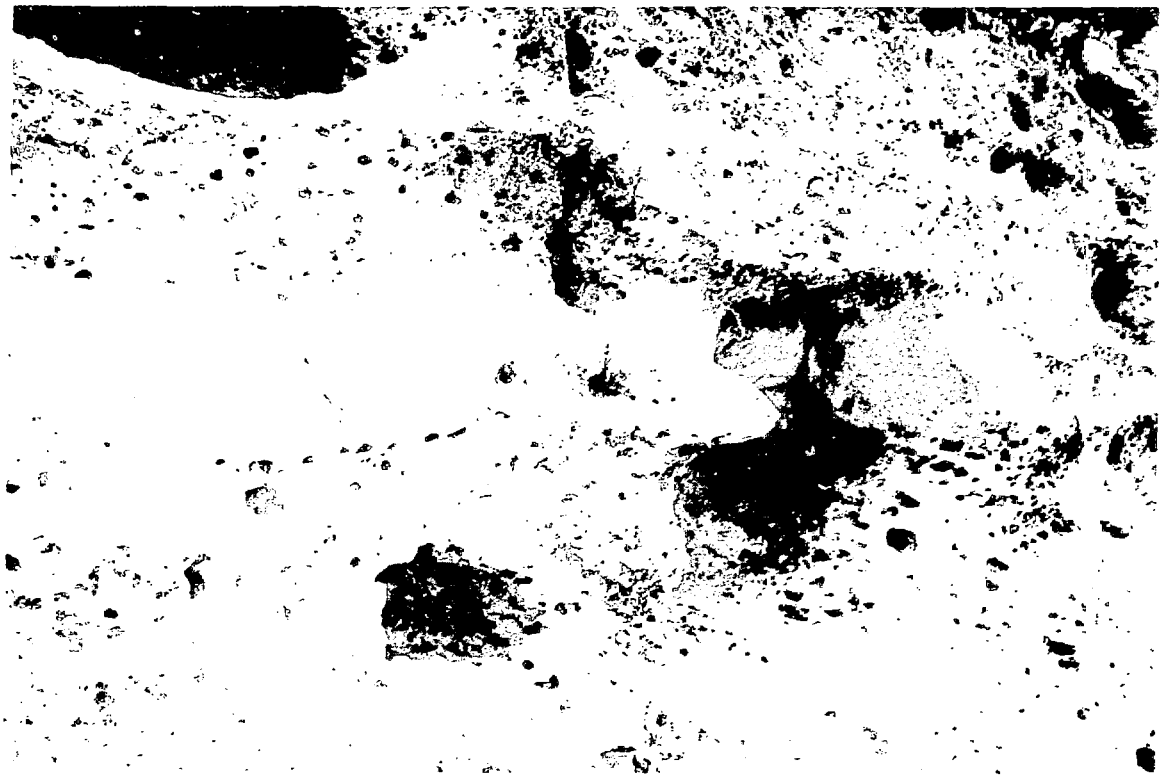

Fig. 10.
Thin flow units in the upper part of cooling unit one. Individual flow units are 1 to 3 m thick, have well-developed fine-grained basal layers and overlying pumice swarms, but generally lack pyroclastic surge deposits. Lower part of photograph is the upper pumice swarm of a lower flow unit. Middle sequence is one flow unit (1 m thick) and the lower part of a third flow unit is visible in the upper part of the photograph (note pumice-poor, fine-grained basal layer of upper flow unit).

size of lithic fragments and an increase in total percent of crystals. Lithic fragments are entirely volcanic flow rocks and some fragments are as large as 0.4 m. This crystal and lithic zone has been described by Smith and Bailey (1966). They suggest that the horizon represents an episode of caldera collapse during the development of Valles Cauldron.

B. Composite Column Two

Composite column two shows the stratigraphy of the Bandelier Tuff for the upper parts of Bayo, Pueblo, and Los Alamos Canyons (Fig. 3); the major stratigraphic features for these areas are illustrated on Fig. 12. In this section

Fig. 11.

Contact between cooling unit one and cooling unit two near the lower part of Ancho Canyon. Note internal pumice swarm within the fine-grained basal layer of the upper flow unit. The lower pyroclastic surge deposits crop out as three distinct zones below the thick fine-grained basal layer. These zones are separated by both pumice poor and pumice rich zones suggesting the presence of secondary flow zones or emplacement surges within the pyroclastic surge horizon. The basal contact of the upper flow zone is defined at the bottom of the basal fine-grained layer. Total outcrop width approximately 4 m.

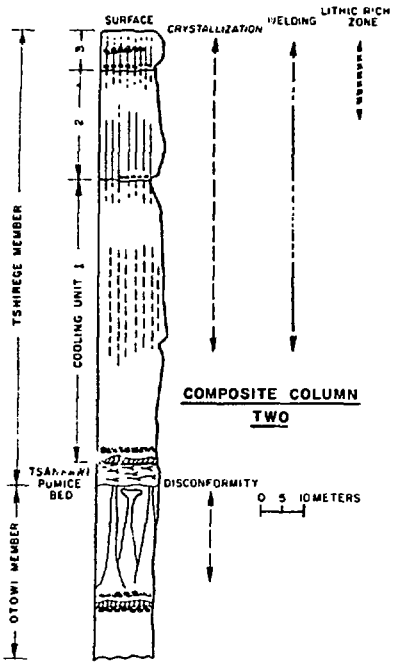


Fig. 12.
Primary depositional features and secondary features of the Bandelier Tuff, composite column two. Refer to Fig. 4, for explanation of symbols.

of the report, physical changes in the Tuff from the area of composite column one to composite column two are emphasized. Much of the stratigraphic descriptions of composite column one apply to column two and are not repeated.

1. Otowi Member

The Otowi Member is exposed only at several localities in the lower parts of canyon walls within the area of composite column two. Exposed sections include the upper part of the ash-flow sequence; the Guaje Pumice Bed is not exposed. The sequence comprises lithic rich, ash-flow tuff. The deposits are unwelded even in the most proximal sections of the column area. The upper contact of the Otowi Member is an erosional surface overlain by basal deposits of the Tshirege Member.

2. Tshirege Member

Tsankawi Pumice Bed

The Tsankawi Pumice Bed coarsens slightly from column one to column two (increase in maximum size of pumice and lithic fragments). Locally there is an increase in the thickness and occurrence of reworked deposits within the section. However these deposits may be formed during very brief time intervals and thus probably do not record significant pauses in eruptive activity. Moreover the local thickness of reworked debris is strongly controlled by paleotopographic irregularities.

3. Ash-flow Sequence

There are significant variations in the occurrence and stratigraphic position of secondary features within the area of composite column two. Three cooling units are present (Fig. 12). The cooling units are somewhat thicker than the same cooling units of composite column one. However thickness

variations due to local paleotopographic irregularities are of considerably greater magnitude than gradational lateral variations in thickness. The erosional notch produced by the onset of vapor-phase crystallization remains a prominent horizon in the section (Fig. 12). The thickness of the zone of partial welding increases in all the cooling units. For cooling unit one, the zone of partial to incipient welding extends upward through nearly the complete cooling unit. There is not, however, a notable change in the maximum degree of welding (determined by porosity estimations). For cooling units two and three, there is both an increase in the thickness of welding zones and a marked increase in the maximum degree of welding. The development of columnar jointing within the cooling units varies with the changes in welding zones. For example, cooling joints extend over a broader zone of cooling unit one. These joints are widely spaced and less sharply developed than joints in cooling unit one in composite column one. In fact, the prominent, strongly jointed zone of cooling unit one in the area of column one (unit 1b of Griggs, 1964, and Baltz and others, 1962) cannot be recognized within much of the area of composite column two. Cooling joints within cooling unit two and three are strongly developed (Fig. 12).

The variations in secondary features of composite column two are consistent with the probable increased emplacement temperature of the more proximal deposits. Moreover the changes in development of secondary features are more pronounced for cooling units two and three than one. This is consistent with an increase in the emplacement temperature of ash-flow deposits upward in the stratigraphic section (Smith and Bailey, 1966).

There are significant variations in the occurrence of primary depositional features of composite column two. The flow-unit textural zones of the basal deposits of the ash-flow sequence of the Tshirege Member are well developed. These textural zones are laterally persistent and are important stratigraphic markers. The thin flow units present in the upper part of cooling unit one in composite column one (Fig. 4), are not present in composite column two (Fig. 12). The contact between cooling unit one and cooling unit two is not a prominent flow unit contact. It is marked only locally by poorly developed, lenticular pumice swarms.

There are several explanations for the lateral changes, from composite column one to composite column two, in development of primary depositional

features. The development of textural zones within a pyroclastic flow unit implies sorting of particles. Sorting is determined primarily by the fall velocity of transported particles, turbulent diffusion within the transporting media, mechanisms of particulate transport, and shear stress at the media-depositional surface interface (boundary effects). There are two types of sorting: local sorting and progressive sorting (Brush, 1965). Changes in textural zones of a flow unit may reflect the action of progressive sorting. That is, there may be a transport time (distance control) for a flow to develop textural zonations. In this manner, textural zones of an individual flow unit would be poorly developed for proximal deposits (short transport time) and become progressively more developed for distal deposits (increased transport time). A second factor may be paleotopography. Distinct paleotopography such as an existing stream drainage has the effect of guiding or channeling a density flow resulting in an increased particle concentration within the channeled part of the flow. A high particle concentration results in a decrease in the ability of a flow to sort due to the physical effect of increased particle collisions (Middleton, 1969). Thus the areas of composite column two lacking flow unit zones may have been deposited within channel interiors. Analogous effects of channeled topography on base-surge flow and resulting deposits have been described by Crowe and Fisher (1973) and Schmincke and others (1975).

C. Composite Column Three

Composite column three was constructed for a distal part of the Bandelier Tuff, within Ancho and Water Canyons (Fig. 3). Stratigraphic features of the Bandelier Tuff for this area are shown on Fig. 13. The stratigraphy is similar to composite column one (Fig. 4). However there are important local variations in the Tuff within the area of composite column three due to:

(1) Major paleocanyons trending roughly parallel to present canyons were incised into deposits of the Otowi Member before deposition of the Tshirege Member. The ash-flow sequence of the Tshirege Member thickens within and thins on the margins of the paleocanyons.

(2) There was a major topographic high produced by the basalts of Santa Ana Mesa and Cerros del Rio local to and extending to the north and south of White Rock (Fig. 3). The Bandelier Tuff thins and locally pinches out onto the basalt paleohigh.

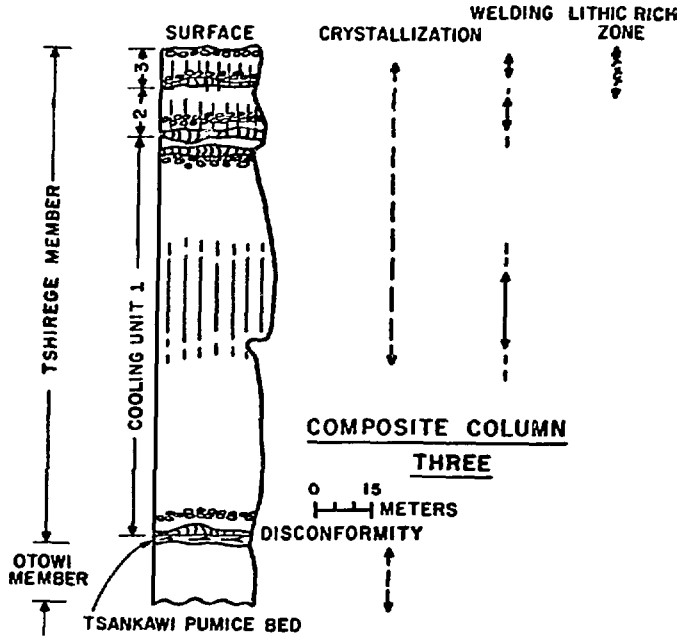


Fig. 13.

Primary depositional features and secondary features of the Bandelier Tuff, composite column three.

1. Otowi Member.

The Otowi Member is present as small erosional remnants within Ancho and Water Canyons. In most places, the Otowi Member was entirely removed by erosion and the Tshirege Member rests directly on basalt. Only the ash-flow sequence of the Otowi Member is exposed in the area of composite column three. The deposits of this sequence are unwelded, lithic rich tuff to lapilli tuff similar to the described deposits of composite columns one and two.

2. Tshirege Member.

a. Tsankawi Pumice Bed.

The Tsankawi Pumice Bed is exposed at many localities within composite column three. Here the deposits are thin (10-40 cm), generally lack reworked horizons and probably record only a single ash-fall eruptive event. The lateral changes in the Tsankawi Pumice Bed probably reflect depositional control by prevailing winds during the Plinian eruptions. We are in the process of

determining detailed size and thickness patterns of the Tsankawi for the eastern Jemez Mountains.

b. Ash-Flow Sequence

Secondary features of the ash-flow sequence of composite column three are closely similar to those of composite column one. The stratigraphy and secondary features of the former area are shown on Fig. 13 (compare with Fig. 4). However, the ash-flow sequence thickens markedly within the axis of paleocanyons. This thickening is most pronounced for cooling unit one as the flow units of the sequence partly to completely filled the irregular topography. Successive cooling units show less pronounced thickness variations. The thickening of cooling unit one resulted in two major effects. First, there is an increase in the thickness of the zone of partial welding in the cooling unit due to increased heat retention. For example, within the axis of a narrow paleocanyon near the terminus of Ancho Canyon, the zone of partial welding extends from 10 m above the base of cooling unit one upwards to near the top of the cooling unit (here the cooling unit top is marked by a well- developed upper-pumice swarm). Second and as a result of the increased welding effects, cooling joints extend throughout a wider zone of cooling unit one. In direct contrast to the paleocanyon sections, the ash-flow sequence exhibits the opposite effects where it thins onto the basalt paleohigh. Here as a result of decrease heat retention and decreased cooling unit thickness, the zones of welding thin and in most cases, cooling joints are absent or are poorly developed. Near the western edge of White Rock, cooling unit one is unwelded through the entire section and both cooling unit one and two lack vapor-phase crystallization.

Primary depositional features of composite column three are similar to composite column one (see Figs. 4 and 13). There are distinct flow unit zones at the base of cooling unit one and thin flow units within the upper part of the unit. The contact between cooling unit one and cooling unit two is a prominent flow-unit contact. Flow unit textural zones are well developed at the base and within the interior of cooling unit three. Thus cooling unit three is a multiple-flow, cooling unit.

## V. GEOCHEMISTRY

The geochemical sampling procedures for the project were designed to provide specific data concerning the geochemical suitability of the Bandelier Tuff as a waste repository medium. The sampling procedures were chosen to investigate: 1) background geochemistry of the Tuff; 2) geochemical variability within the Tuff; and 3) chemical reactivity of the Tuff to natural alteration processes. The data, when completely determined, will allow consideration of possible interaction of the natural system, the Tuff, with waste.

Two types of geochemical samples were collected for the project. The first type includes samples obtained from parts or complete sections of specific stratigraphic units. Data from these samples can be used to establish background chemistry and test for variability of chemical components within the Tuff. The second type includes samples of altered Tuff and contiguous wall-rock. These samples can be used to determine mass transfer by alteration processes affecting the Tuff.

Channel samples are continuous, vertical scrappings, or chippings of unaltered rock obtained through an entire designated section. The purpose of a channel sample is to obtain an unaltered and homogenized sample that is representative of a selected unit or interval. The analytical results from the sample provide a general background level of elemental concentrations that constitute a base level for comparison with analytical results from other types of samples. Channel samples were collected from composite columns one and three.

Pumice samples were collected every 3 m throughout sections of the Tuff where the rock was not too indurated to sample. These samples must closely represent the chemistry of the parent magma because pumice is a chilled, uncontaminated sample of the magma and the pumice chemistry has not been modified by transport processes. Bulk rock samples were collected every 3 m regardless of induration. These samples provide rock for thin sections, polished sections or material for uses other than rapid geochemical analyses.

A well-exposed flow-unit in the Tshirege Member was sampled in the area of composite column three. This flow-unit, from a distal area of the Tuff, is both unwelded and unaffected by vapor-phase crystallization. The flow had been eroded so an unknown amount of the upper part is not extant and could not be sampled. The entire remainder, which includes well-developed textural zones of

the basal part of a flow-unit (Fig. 3), was sampled in 5-cm increments through a 260-cm-vertical section. The intent of this sampling was to analyze for geochemical homogeniety within a flow-unit. These data are necessary before proceeding with other types of geochemical investigations that assume flow-unit geochemical homogeniety, such as the determination of exchange of elements between shards and matrix by scanning electron microscope x-ray mapping. Moreover, the flow-unit contact is the same stratigraphic horizon, described in a later section of the report, exposed in the waste disposal site at TA-54.

The results of geochemical analysis of alteration material and the adjacent wall-rock are necessary to determine mobile elements, define the mechanism of transport and to determine the composition of alteration products. Joint-fill material and paleo-aquifer ledges were sampled in 5-cm increments, where applicable, and the surrounding wall-rock was sampled for 1 m in 10-cm increments. A wide variety of joint-fill material was collected and a total of five alteration ledges in Ancho Canyon and two in the area of composite column one were sampled.

At the time of writing, 100 samples have been prepared and submitted to Group P-2, Research Reactor Experiments, for analyses. Results have been returned for 50 samples. Major and trace element abundances for the samples and sample descriptions are presented in Appendixes 1 and 2. Elemental analyses were by neutron activation; uranium was determined by delayed neutron counting. Appendix 3 lists the detection limits of the two techniques as well as the counting group of each element. The short count analyses were lost for sample 4341.3.

We have just initiated examination of the analytical results and have not yet plotted the data versus appropriate chemical parameters. At present, we have only checked the results for obvious anomalies. These results of this examination are presented in Table I.

## VI. PETROGRAPHY

Detailed petrographic studies of the Bandelier Tuff have been partly completed. We have determined representative modes for most of the units, and determined feldspar compositions and glass compositions by electron microprobe for some of the units.

TABLE I: Anomalous concentrations of major oxides and elements in some samples of Bandelier Tuff. Samples are enriched unless underlined, which indicates depletion. Values are in weight percent.

| Sample No. | 4250.1 | 4253.3 | 4323.3 | 4325.3 | 4326.3 |
|---|---|---|---|---|---|
| $Al_2O$ | 27.21 | | 10.68 | | 5.22 |
| CaO | 7.56 | 1.37 | | 2.90 | |
| Cl | 0.02 | 0.79 | | | |
| MgO | 3.20 | | | 1.20 | |
| $K_2O$ | | | | 1.94 | |
| $Na_2O$ | 0.43 | | | 2.93 | |
| $TiO_2$ | 1.02 | | | | |

TABLE I. Anomalous concentrations of trace elements in some samples of Bandelier Tuff. Samples are enriched unless underlined, which indicates depletion. Values are in ppm.

| Sample No. | Sb | Ba | Co | Cu | Rb | Sr | V | W |
|---|---|---|---|---|---|---|---|---|
| 4250.1 | | 2630.0 | | | | | 253.0 | |
| 4257.3 | | | | | 149.0 | | | |
| 4267.1 | | | | | | | | 115.0 |
| 4267.2 | 8.9 | | | | | | | |
| 4274.1 | | | | | | | | 105.0 |
| 4277.1 | | | | | 129.0 | | | |
| 4280.1 | | | | | 142.0 | | | |
| 4281.1 | | 168.0 | | | | | | 269.0 |
| 4282.1 | | 103.0 | | | 136.0 | | | 158.0 |
| 4283.1 | | | | | 129.0 | | | |
| 4284.1 | | | | | 118.0 | | | 131.0 |
| 4285.1 | | | | | 119.0 | | | 147.0 |
| 4291.1 | | | | | 114.0 | | | |
| 4317.3 | | | | | 127.0 | | | |
| 4318.3 | | | | | 143.0 | | | 107.0 |
| 4323.3 | | | | 145.0 | 154.0 | | | |
| 4324.3 | | | | | 104.0 | | | |
| 4325.3 | | | | | 65.1 | 1190.0 | | 117.0 |
| 4327.3 | | 130.0 | | | | | | 120.0 |
| 4331.3 | | | | | | | | 118.0 |
| 4335.3 | | 130.0 | | | | | | 248.0 |
| 4338.3 | | | | | 134.0 | 835.0 | | |
| 4340.3 | | | | 278.0 | | | | |

A. Otowi Member

In order to examine changes in glass compositions and phenocryst assemblages, pumice clasts from successive stratigraphic horizons in the Otowi Member were examined. The pumice clasts consist of vesiculated rhyolite glass with total phenocryst contents ranging from trace amounts to 13 modal %. Modal mineralogy of pumice clasts from the Otowi Member (ash-flow sequence) are summarized in Table II. Primary phenocryst phases include sanidine and quartz with trace amounts of orthopyroxene and iron-titanium oxides. Sanidine phenocrysts are anhedral to euhedral and range in size from 0.1 mm to 2.0 mm. Some of the larger phenocrysts exhibit Carlsbad twinning and are partly resorbed. Sanidine compositions were determined by electron microprobe and are listed in Appendix IV. These are sanidines that plot compositionally near the anorthoclase border on the ternary diagram of Ab-Or-An (Deer and other, 1966). There is no apparent change in composition of the sanidines through the Otowi section. In general crystal cores are slightly more potassic than crystal rims (Appendix IV). Quartz phenocrysts are subhedral to euhedral and are up to 2.0 mm in diameter. Many of the crystals are partly to strongly resorbed.

Composition of glass in the pumice fragments of the Otowi Member (ash-flow sequence) were analyzed by electron microprobe (Table III). The glass compositions are rhyolitic with total alkalies averaging approximately 7.8 wt %, and moderate alumina (approximately 11.5 to 12.0 wt %). There are no recognizable systematic variations in the glass compositions through the ash-flow sequence. For comparison, glass compositions are higher in $K_2O$ and contain lesser amounts of $Al_2O_3$, FeO, and $Na_2O$ than the channel sample of the ash-flow sequence of the Otowi Member (Appendix I).

B. Tshirege Member

Modal mineralogy of representative samples of the ash-flow sequence of the Tshirege Member are shown in Table IV; alkali-feldspar compositions are shown in Appendix IV.

We have not yet attempted to systematically describe the petrography of the Tshirege Member. Mineralogical variations are complex and require careful correlation with stratigraphic units. The mineralogy of the Tshirege Member has been briefly described by Smith and Bailey (1966). They noted significant variations in the composition of alkali feldspars and in the total abundance and proportions of major phenocryst phases with stratigraphic position within the ash-flow sheet (Smith and Bailey, 1966, their Fig. 13). These variations are

TABLE II: Modal Mineralogy of Pumice Clasts, Ash-Flow Sequence of the Otowi Member, Composite Column One.

| Sample No. 77042 | 17.2 | 18.2 | 19.2 | 20.2 | 21.2 | 22.2 | 24.2 | 25.2 | 27.2 |
|---|---|---|---|---|---|---|---|---|---|
| Height above base | 3.7m | 5.5m | 7.3m | 9.1m | 11m | 12.8m | 16.5m | 18.3m | 19.8m |
| Glass | 47.7 | 46.9 | 42.7 | 47.7 | 47.7 | 37.7 | 49.3 | 47.4 | 40.7 |
| Vesicles | 50.7 | 50.8 | 57.3 | 46.3 | 48.7 | 57.0 | 42.7 | 49.0 | 46.7 |
| Sanidine | 1.0 | 1.9 | Tr | 5.7 | -- | 6.3 | 7.7 | 3.6 | 8.7 |
| Quartz | 0.7 | 0.3 | -- | -- | 1.9 | -- | -- | Tr | 4.0 |
| Opx | -- | -- | -- | -- | 0.3 | -- | 0.3 | -- | -- |
| Magnetite | -- | -- | -- | -- | -- | Tr | Tr | -- | -- |
| Total # Points | 300 | 309 | 300 | 300 | 302 | 300 | 300 | 302 | 300 |

| Sample No. 77042 | 30.2 | 31.2 | 33.2 | 34.2 | 35.2 | 27.2 | 38.2 | 39.2 | 40.2 |
|---|---|---|---|---|---|---|---|---|---|
| Height above base | 24.4m | 25.9m | 30.5m | 32.0m | 33.5m | 36.8m | 38.3m | 40.1m | 41.7m |
| Glass | 39.0 | 43.1 | 43.3 | 48.0 | 45.2 | 60.3 | 45.6 | 42.1 | 40.0 |
| Vesicles | 52.0 | 51.0 | 53.3 | 47.0 | 49.2 | 38.3 | 44.3 | 56.7 | 49.3 |
| Sanidine | 8.7 | 4.9 | 3.3 | 4.3 | 3.9 | 1.3 | 8.8 | 0.7 | 6.0 |
| Quarta | 0.3 | 1.3 | -- | 0.77 | 1.0 | -- | 1.9 | -- | 4.7 |
| Opx | Tr | -- | -- | -- | 0.3 | -- | -- | -- | -- |
| Magnetite | -- | -- | -- | -- | 0.3 | -- | -- | -- | -- |
| Total # Points | 300 | 304 | 300 | 302 | 305 | 300 | 307 | 300 | 250 |

TABLE III: Electron Microprobe Analyses of Glass Compositions, Otowi Member.

| Sample No. | 77.04216.2 | 77.04220.2 | 77.04232.2 | 77.04236.2 | 77.04240.2 |
|---|---|---|---|---|---|
| $SiO_2$ | 73.78 | 74.03 | 73.59 | 73.92 | 74.94 |
| $TiO_2$ | 0.10 | 0.08 | 0.10 | 0.11 | 0.07 |
| $Al_2O_3$ | 11.74 | 11.92 | 12.05 | 11.73 | 12.05 |
| *FeO | 1.15 | 1.06 | 1.11 | 1.09 | 1.14 |
| MgO | 0.05 | 0.04 | 0.04 | 0.05 | 0.03 |
| CaO | 0.30 | 0.29 | 0.29 | 0.29 | 0.25 |
| $Na_2O$ | 3.38 | 2.82 | 3.23 | 2.95 | 3.29 |
| $K_2O$ | 4.42 | 4.68 | 4.65 | 4.89 | 4.70 |
| F | 0.1 | 0.09 | 0.06 | 0.04 | 0.05 |
| TOTAL | 95.02 | 95.01 | 95.12 | 95.07 | 96.52 |
| No. of Average Analyses | 6 | 6 | 6 | 5 | 6 |

*Total iron as FeO.

reflected in the modes we determined (Table IV) and in electron microprobe determinations of feldspar compositions (Appendix IV).

## C. Particle Morphology and Granulometry

The nature of pumice and shard shapes controls the surface area within a designated volume of the Bandelier Tuff. The total surface area strongly controls reaction rates of alteration processes. In this section of the report we describe pyroclast morphology from the Plinian air-fall deposits (Guaje Pumice Bed and Tsankawi Pumice Bed) and from unconsolidated parts of the ash-flow sequences of the Otowi and Tshirege Members. For some of the samples we have calculated approximate surface areas. Additionally we present the results of preliminary granulometric analyses. These data provide background information necessary for examination of alteration processes effecting the Bandelier Tuff and potential interaction with radioactive waste.

### 1. Particle Morphology

Results from the analyses of particle shards are presented in Table V. Pyroclast types illustrated in the figures (Figs. 14-17) are described below.

TABLE IV: Modal Mineralogy of the Ash-Flow Sequence, Tshirege Member, Composite Column One.

| | Lower, Unwelded Zone, Cooling Unit One | | | | | | | | Zone of Partial Welding, Cooling Unit One | | | | | |
|---|---|---|---|---|---|---|---|---|---|---|---|---|---|---|
| No. 77042___ | 64.1 | 65.1 | 66.1 | 67.1 | 68.1 | 69.1 | 70.1 | 71.1 | 72.1 | 73.1 | 74.1 | 75.1 | 76.1 | 78.1 |
| Unit, Pt. of Measurement | Base | | | | | | | | | | | | | |
| "Matrix" | 22.7 | 7.0 | 8.6 | 11.3 | 13.8 | 18.3 | 20.6 | 54.0 | 76.7 | 72.0 | 75.7 | 71.1 | 58.3 | 55 7 |
| Shards | 59.0 | 31.7 | 41.6 | 28.0 | 27.4 | 42.3 | 25.2 | 8.3 | 11.7 | 14.0 | 10.7 | 6.9 | 12.3 | 11.3 |
| Pumice | 14.3 | 43.0 | 35.0 | 39.3 | 32.1 | 25.0 | 27.6 | 4.7 | 3.3 | 2.7 | 1.3 | 4.6 | 13.0 | 5.3 |
| Sanidine | 2.3 | 12.3 | 10.9 | 13.7 | 17.1 | 10.7 | 13.3 | -- | 0.7 | 1.3 | 4.7 | 1.3 | 0.3 | 2.3 |
| Quartz | 0.7 | 4.0 | 2.0 | 6.3 | 3.8 | 3.0 | 10.6 | 6.7 | -- | -- | 0.3 | 0.3 | 0.7 | -- |
| Xenoliths | 1.0 | 1.3 | 1.7 | 1.3 | 5.6 | 3.0 | 1.0 | 0.7 | 7.0 | 10.0 | 5.7 | 14.4 | 13.7 | 25.0 |
| Plagioclase | -- | 0.7 | 0.3 | -- | 0.3 | -- | -- | -- | -- | -- | -- | 0.3 | 0.3 | -- |
| Hornblende | -- | -- | 0.3 | -- | -- | -- | -- | -- | 0.7 | -- | -- | 0.3 | 1.0 | 0.3 |
| Sl. altered shards | -- | -- | 0.3 | -- | -- | -- | 1.3 | 23.3 | -- | -- | -- | -- | -- | -- |
| Total # Grains | 300 | 300 | 303 | 300 | 340 | 300 | 301 | 300 | 300 | 300 | 300 | 305 | 300 | 300 |

| | Upper Unwelded Zone, Cooling Unit One | | | | | | Zone of Partial Welding, Cooling Unit Two | | | Zone of Partial Welding, Cooling Unit Three |
|---|---|---|---|---|---|---|---|---|---|---|
| No. 77042___ | 80.1 | 81.1 | 82.1 | 83.1 | 84.1 | 85.1 | 87.1 | 88.1 | 89.1 | 91.1 |
| Unit, Pt. of Measurement | | | | | | | | | | |
| "Matrix" | 65.1 | 57.7 | 58.7 | 59.3 | 63.0 | 63.3 | 61.3 | 71.3 | 69.0 | 62.0 |
| Shards | 20.9 | 18.3 | 16.7 | 21.3 | 12.7 | 17.7 | 13.3 | 17.0 | 12.7 | 15.7 |
| Pumice | 1.0 | 3.0 | 4.7 | 2.0 | 6.3 | 6.7 | 2.7 | 2.3 | 0.3 | 2.3 |
| Sanidine | -- | -- | -- | -- | -- | 0.3 | -- | 0.3 | -- | -- |
| Quartz | -- | 00 | -- | -- | -- | -- | -- | -- | -- | -- |
| Xenoliths | 12.3 | 20.7 | 18.7 | 17.0 | 18.0 | 12.0 | 22.3 | 11.0 | 17.7 | 19.7 |
| Plagioclase | 0.3 | -- | 0.3 | 0.3 | -- | -- | -- | -- | -- | -- |
| Hornblende | -- | -- | 0.7 | -- | -- | -- | 0.3 | -- | 0.3 | -- |
| Sl. altered shards | -- | -- | -- | -- | -- | -- | -- | -- | -- | -- |
| Total # Grains | 301 | 300 | 300 | 300 | 300 | 300 | 300 | 308 | 300 | 300 |

TABLE V: Surface Area Calculations, Unwelded Ash-Flow Deposits, Tshirege Member

| Sample No. | Description | Surface Area per $cm^3$ (in $cm^2$) |
|---|---|---|
| 77.04264.1 | Unwelded base of cooling unit 1 | 521.8 |
| 77.04265.1 | 1.8 m above base of cooling unit 1 | 641.9 |
| 77.04266.1 | 3.7 m above base of cooling unit 1 | 572.3 |
| 77.04267.1 | 5.5 m above base of cooling unit 1 | 571.1 |
| 77.04268.1 | 7.4 m above base of cooling unit 1 | 594.5 |
| 77.04285.1 | 17.4 m above base of cooling unit 2 | 713.0 |

a. Crystal Pyroclasts.

Phenocrysts with bubble-wall textures. These include sanidine or quartz phenocrysts partly to completely encased in a glass coating. The coating is vesiculated, with 150- to 300-μm diam flattened ovoid vesicles (Fig. 14). The large and intermediate axes of the vesicles are parallel to phenocryst grain surfaces.

b. Pumice Pyroclasts.

Pumice with thin elongate vesicles. These consist of equant to elongate, angular pyroclasts. Vesicles are thin with high (>50:1) aspect ratios (Fig. 15). Megascopically these pyroclasts have a "silky" appearance. Some of the pumices have flattened, elongate surface cavities up to 300 μm long and 100μm wide. These are due to coalesced vesicles; septa within these cavities are remnants of collapsed vesicle walls.

Pumice with equant to slightly elongate ovoid vesicles. These contain vesicles with aspect ratios ranging from 30:1 to 1:1 (elongate ovoids to spheroidal shapes). Vesicle walls are deformed and have a polygonal apparance. Vesicle diameters range from 100 to 500 μm (Fig. 16).

Finely vesicular, massive pumice pyroclasts. These pyroclasts are completely vesiculated with spherical to slightly ovoid vesicles and thick vesicle walls. There are two distinct vesicle diameters; 20 to 80 μm and 5 to 15 μm. Most of the pyroclasts have equant, subangular shapes (Fig. 17).

2. Surface Area Calculations

Approximate surface area calculations were determined assuming high porosity and permeability and therefore complete contact by the fluid media with particle surfaces. Surface areas of particles were calculated for grains of average diameter within chosen size fractions and surface area per cubic centimeter was determined. Grain-size analyses were used to determine surface area per cubic meter of each designated unit. Results of the calculations are listed in Table V.

3. Granulometry

Unconsolidated samples from the unwelded zones of cooling unit one of the Tshirege Member were collected for grain-size analysis (Table VI). Each sample was gently sieved and washed through sieve stacks using a 0.5$\phi$ sieve interval (range - 2$\phi$ to 4.5$\phi$ ). Particular care was taken to not abrade delicate pumice fragments and bias the analysis. The size fraction smaller than 4.5$\phi$ for two of the samples was analysed using a sedimentation (pipette) method. Nearly all of the samples fall within the category of coarse ash and all are very poorly sorted, with the exception of the bedded portion of the base of cooling unit one (poorly sorted, Figs. 19, 20). In a plot of mean grain size versus sorting (Fig. 18), all of the samples fall within the ash-flow category of Walker (1971). The bedded sample from the base of cooling unit one plots near the boundary of the flow field (Fig. 18).

## VII. APPLICATIONS TO WASTE MANAGEMENT STUDIES

Direct applications to waste management studies of results summarized in this report include information for several broad areas:

- Supportative stratigraphic studies
- Physical and structural controls of waste migration paths
- Geochemistry of the Bandelier Tuff

### A. Supportative Stratigraphic Studies

The most useful field tool in studying complex ash-flow sheets is the cooling unit (Smith, 1960a). We have defined three cooling units within the

TABLE VI: Granulometry of tephra from the Tshirege Member, Unwelded Zones of Cooling Unit One

| Sample No. | Unit | $M_Z\phi$ | $M_Z$(mm) | $\sigma$ | Verbal Description of Sorting |
|---|---|---|---|---|---|
| 77.04264.1 | 1A | 4.02 | 0.061 | 1.95 | poorly sorted (ps) |
| 77.04265.1 | 1A | 2.28 | 0.206 | 2.38 | very poorly sorted (vps) |
| 77.04266.1 | 1A | 1.62 | 0.325 | 2.85 | vps |
| 77.04267.1 | 1A | 1.65 | 0.319 | 2.80 | vps |
| 77.04268.1 | 1A | 1.9 | 0.268 | 2.58 | vps |
| 77.04269.1 | 1A | 1.28 | 0.412 | 2.5 | vps |
| 77.04270.1 | 1A | 1.7 | 0.31 | 2.6 | vps |
| 77.04285.1 | 2 | 2.37 | 0.193 | 2.48 | vps |

Note: Statistical parameters of grainsize ($M_Z$=graphic mean, $\sigma$=graphic standard deviation) from Folk, 1965.

Tshirege Member of the Bandelier Tuff. The cooling units are relatively thin toward the margin of the Pajarito Plateau and merge to form a single thick cooling unit near Valles Caldera (west of the area of this report). Cooling units and welding and compaction zones within a cooling unit are not precise stratigraphic markers; their stratigraphic position within an ash-flow sheet will vary laterally. In order to properly use cooling units as mapping units, variations in welding must be understood. Several variables affect welding (Smith, 1960a; Riehle, 1973):

- temperature of the deposits
- Volume and composition of volatiles (controlled by volatile content of the magma, mechanism of eruption and emplacement, and lateral transport distance).
- Ash composition (largely a viscosity effect).
- Lithostatic load (controlled by cooling unit thickness).
- Cooling history (conduction, convection, and radiation).
- Crystallization history (vapor-phase crystallization and devitrification).

For the Bandelier Tuff, the volatile content and ash composition can be reduced to a viscosity effect. Viscosity of glass particles is the major control of the compaction coefficient; it will vary by several orders of

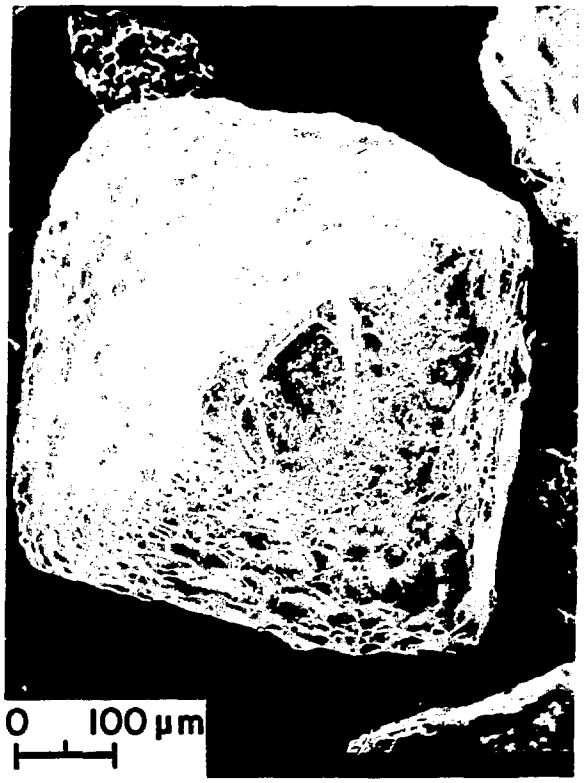


Fig. 14.
Phenocryst from the Guaje Pumice Bed showing bubble wall textures. SEM photograph.

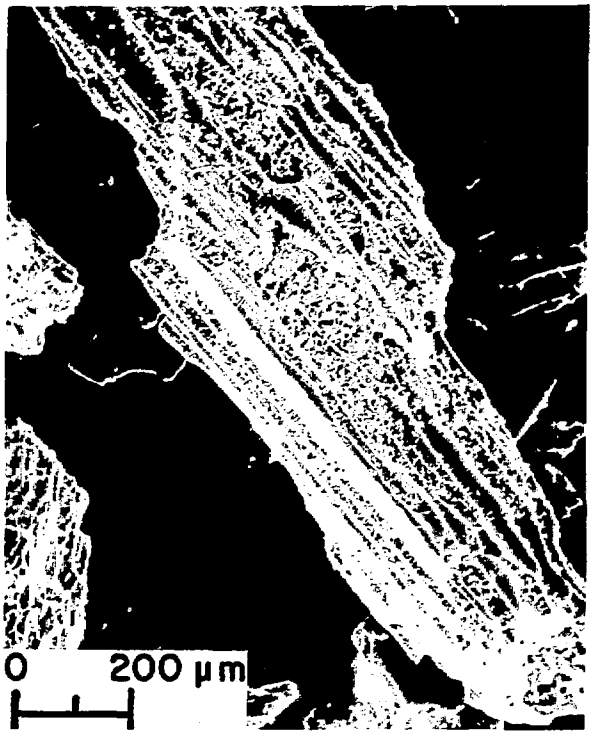


Fig. 15.
Pumice pyroclast with thin, highly elongate vesicles. From the basal unwelded zone of cooling unit one, Tshirege Member. SEM photograph.

magnitude with temperature (Riehle, 1973, Fig. 2). The cooling history is controlled by the mechanisms of cooling; in most cases it is controlled by conduction and radiation (Riehle, 1973). Variations in cooling history will primarily be controlled by initial temperature of emplacement and the thickness of cooling units. The crystallization history will not have a major effect on welding. This is illustrated by two studies. Riehle (1973) suggests that essentially all the heat of an ash flow deposit is contained in the solid phases; heat transferred by escaping volatiles has a negligible effect. Sheridan (1971) has shown, for the Bishop Tuff, that devitrification occurred after welding and compaction and therefore did not affect development of these zones.


Fig. 16.
Pumice pyroclast with equant to ovoid vesicles, from the Tsankawi Pumice Bed of the Tshirege Member. SEM photograph.

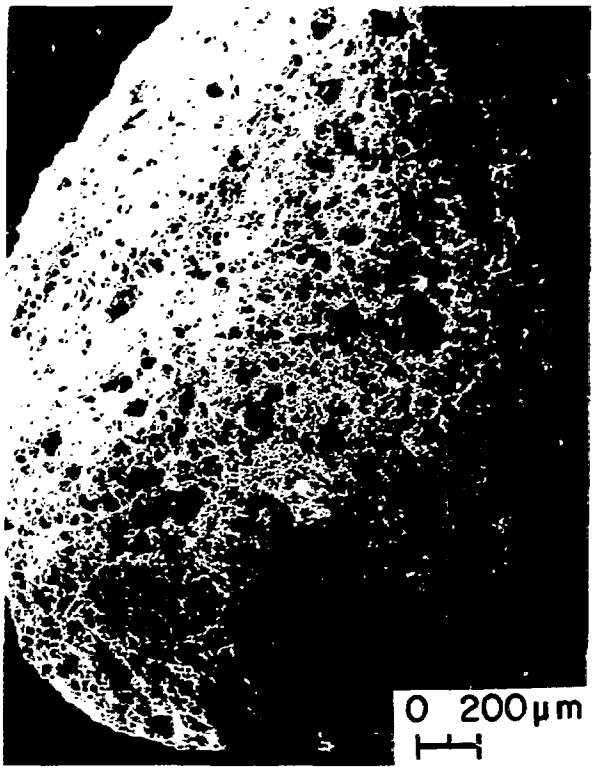


Fig. 17.
Finely vesicular, massive pumice pyroclast from the Tsankawi Pumice Bed of the Tshirege Member. SEM photograph.

Lateral variations in the welding and compaction history of the Bandelier Tuff (cooling unit characteristics) will be controlled primarily by emplacement temperature and lithostatic load. Emplacement temperature is controlled by several variables: (1) Absolute temperature and temperature gradients in the magma, (2) Mechanism of generation of pyroclastic flows (Wilson and Sparks, 1977), and (3) Lateral transport distance. For any single cooling unit, magma temperatures will be relatively constant and the mechanism of generation of pyroclastic flows should show relatively limited variation. Lithostatic load is a function of cooling unit thickness. The latter will vary with: (1) Rate and continuity of eruption (rapid continuous eruption results in thick cooling units), and (2) Distance from the vent source.

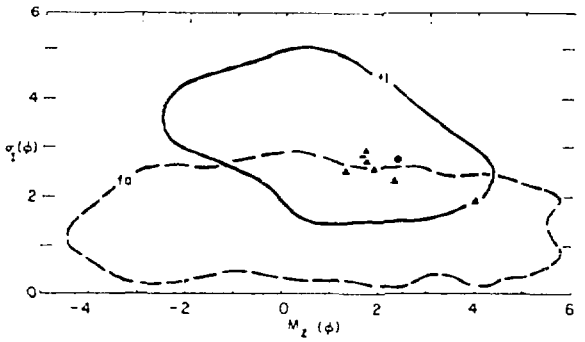


Fig. 18.
Mean-grain size ($M_z$) versus sorting ($\sigma_I$) for selected samples of the Tshirege Member. Ash-flow (Fl) and ash-fall (fa) fields after Walker (1971).

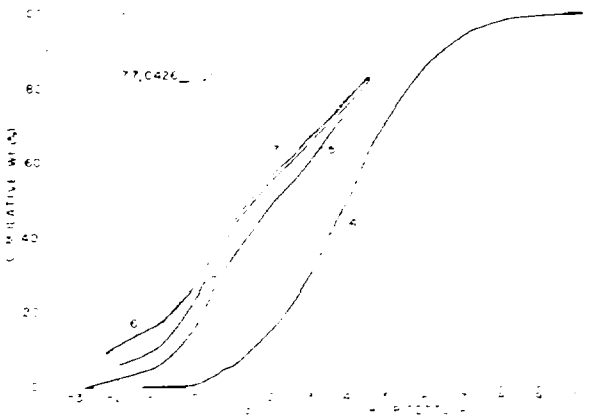

Fig. 19.
Plot of cumulative weight percent versus grain-size (ϕ) for unwelded basal samples of cooling unit one, Tshirege Member.

77.04264.1 Fine-grained basal layer.
77.04265.1 Ash-flow body, 1.8 m above base.
77.04266.1 Ash-flow body, 3.7 m above base.
77.04267.1 Ash-flow body, 5.5 m above base.
77.04268.1 Ash-flow body, 7.4 m above base.

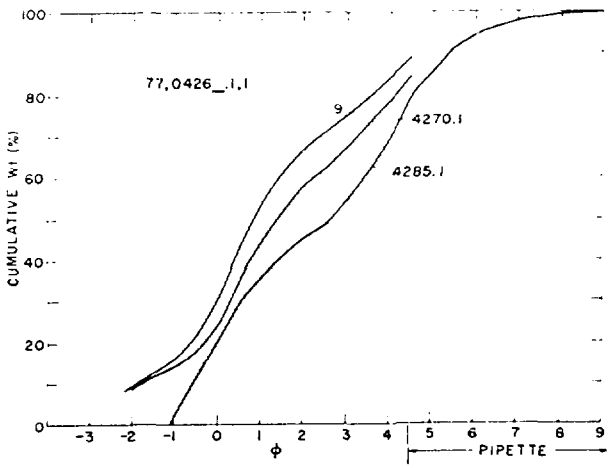


Fig. 20.
Plot of cumulative weight percent versus grain size (ϕ) for unwelded samples of cooling unit one and cooling unit two, Tshirege Member.

77.04269.1 Ash-flow body, 9.2 m above base, C.U.1.
77.04270.1 Ash-flow body, 11.1 m above base, C.U.1.
77.04285.1 Ash-flow body, 17.4 m above base, C.U.2.

Thus it follows that the major control of variation in cooling unit zones will be the distance from the source (see Fig. 1). The important point to this discussion is that as the temperature of emplacement and thickness of an ash-flow cooling unit increases (proximal sections), welding zones will cross stratigraphic horizons. This concept must be applied in mapping cooling units or zones within cooling units.

Several primary depositional features provide stratigraphic markers within the ash-flow sequence of the Tshirege Member. For proximal sections, these include:

- Textural zones that define the flow-unit contact at the base of cooling unit one.
- Pumice swarms (generally poorly developed) near the contact between cooling unit one and two.
- The zone of abundant lithic fragments (volcanic) within cooling unit two and three.

For distal sections, major stratigraphic markers include:

- Textural zones that define the flow-unit contact at the base of cooling unit one.
- Thin flow units in the upper part of cooling unit one.
- Flow unit textural zones that mark the contact between cooling unit one and two.
- Flow unit textural zones at the contact between cooling unit two and three.
- Pumice swarms within cooling unit three.
- The zone of abundant lithic fragments within cooling units two and three.

B. Physical and Structural Controls of Waste Migration Pathways

There are two important factors when considering the geologic controls of migration pathways within the Bandelier Tuff. First, there is significant lateral variability in the Tuff; a detailed evaluation of potential migration pathways is best directed at a site specific level. Second, the value of noting possible migration pathways is minimal without direct hydrologic testing. The significance of identified zones needs to be determined by field hydrology tests.

1. Proximal Sections of the Bandelier Tuff

The hydrologic characteristics of the Bandelier Tuff at proximal sections will be controlled primarily by secondary features and in particular variations in the degree of welding, lateral distribution of welding zones and the occurrence of cooling joints. Porosity can vary on the order of 5 to 50% within welding zones. Zones of maximum welding will have the lowest porosity; zones of partial to no welding will have higher porosity values. Vapor-phase crystallization will reduce porosity and may have important effects on permeability. Predominate flow paths may coincide with boundaries between welding zones where there will be marked contrasts between the porosity and permeability of deposits. The degree of welding directly determines interstitial porosity of ash-flow deposits (Winograd and Thordarson, 1975). In general there is an inverse relationship between degree of welding and porosity. Porosity variations through welding zones of a cooling unit (unwelded to densely welded) range from <5% to as great as 50% (Smith, 1960; Riehle, 1973). This corresponds to bulk density ($gcm^{-3}$) variations on the order of 1.0 to 2.5 (Sheridan and Ragan, 1977). Vapor-phase crystallization will reduce porosity and may reduce permeability. Zones of high-joint density in cooling units may have a significant fracture permeability. These zones coincide with horizons of cooling joint development that in turn are controlled by welding zones within cooling units.

The hydrologic properties of the Bandelier Tuff have not been systematically related to the occurrence of cooling units. However, a considerable amount of information on the hydrologic properties of pyroclastic rocks is known from the Nevada Test Site. In particular the hydrologic properties of ash-flow sheets have been directly related to cooling units (Winograd and Thordarson, 1975). This information has direct application to studies of the Bandelier Tuff.

Welded tuff aquifers in the Nevada Test Site generally are controlled by the zones of partial to dense welding. Here primary cooling joints that are spatially related to the welding zones control transmissibility. For example the water-bearing aquifer below Jackass Flats in the southwestern part of the Nevada Test Site occurs within welded zones of the Topopah Spring Member of the Paintbrush Tuff (Young, 1972). The coefficient of fracture transmissibility for these zones ranges from $10^2$to $10^5$ gallons per day per foot (Winograd and Thordarson, 1975). In contrast unwelded to partially welded zones of ash-flow

sheets in the Nevada Test Site are classified as leaky aquitards; the interstitial coefficient of permeability for these zones ranges from >2 to 0.02 gallons per day per square foot and the coefficient of transmissibility is <100 gallons per day per foot.

The occurrence of major joint systems within the Bandelier Tuff in the Pajarito Plateau is shown on the composite stratigraphic column (Figs. 4, 12, and 13). A few comments on the geometry of joint systems within the Bandelier Tuff are important. There are two types of joint systems present; tectonic joints and cooling joints. Cooling joints are spatially related tc welding zones within a cooling unit. They occur as columnar joint sets that develop perpendicular to isothermal surfaces. Local disturbances in the cooling regime of an ash-flow deposit (for example paleotopography, fumarolic pipes) distort the distribution of isotherms and effect cooling-joint geometry. For example, Sheridan (1971) describes jointing in the Bishop Tuff that in part developed as a result of disturbances of isothermal surfaces due to the formation of large fumarolic pipes. This is an important example of lateral variability in cooling joint geometry. Similar variations are present within the Bandelier Tuff. Thus it is critical to determine the origin and geometry of joint sets within and adjacent to waste disposal sites.

2. Distal Sections of the Bandelier Tuff

Welding zones in distal sections of the Bandelier Tuff progressively thin except in areas of significant paleotopography. Zones of cooling joint development provide continued control of hydrologic properties. Additionally, some migration pathways in distal sections of the Tuff will be controlled by primary depositional features.

Radioactive waste material is buried at shallow levels (near surface) in the Tuff. Thus depositional features in the upper part of the section of the Tshirege Member are probably of prime importance at waste disposal pits. Here we emphasize several horizons:

- Thin-flow units in cooling unit three.
- The flow-unit contact between cooling unit one and cooling unit two.
- Thin-flow units in the upper part of cooling unit one.

There are significant differences in the physical properties of deposits within textural zones of a flow unit (Fig. 3). These physical differences may be important in controlling migration pathways and in particular the contacts

between textural zones. For example, pyroclastic surge deposits are well sorted and laminated (Walker, 1971; Sparks and others, 1973; Crowe and Fisher, 1973). These properties may result in high permeability. In contrast the fine-grained basal layer is poorly sorted and massive; these deposits may have low permeability.

These considerations suggest that attention needs to be directed not only to the presence of flow units within the Tuff but also to textural zones within the flow units. For example, Purtymun (1973) has described the underground migration of tritium from storage shafts within Technical Area 54 (TA-54). He suggested that tritium preferentially followed the contact between two ash flows. We have briefly examined this contact in cliff sections adjacent to TA-54 and in waste burial pits at the site. The described contact is the contact between cooling unit one and cooling unit two. It exhibits well developed flow-unit textural zones that are typical of distal sections of this unit. Purtymun (1973, p. 3-4) notes that a westward assymmetry in isotritium contours is due to increased migration rates along a "thickening of the layer of reworked tuff lying along the contact ....." The "reworked tuff" is pyroclastic surge deposits that form the basal part of a flow unit of cooling unit two. The surge deposits may be a preferential migration pathway although additional pathways may exist due to the presence of the following textural features:

- A distinct pumice swarm at the top of the lower flow unit.
- The fine-grained basal layer overlying the pyroclastic surge deposits.
- A thick pumice swarm overlying the fine-grained basal zone.

Hydrologic properties of deposits referred to as the bedded-tuff aquifer have been examined at the Nevada Test Site (Winograd and Thordarson, 1975). These deposits include air-fall tuff, reworked tuff and thin primary flow units containing notable thicknesses of pyroclastic surge deposits. The hydrologic properties of these rocks thus have application to studies of the Bandelier Tuff. Unaltered sections of bedded tuff at the Nevada Test Site have an average interstitial porosity of 40%; measured interstitial permeability values range from 0.07 to 4.1 gallons per day per square foot (Thordarson, 1965). Coefficients of transmissibility for these rocks as determined from pumping tests range from 200 to 1 000 gallons per day per foot (Winograd and Thordarson, 1975).

C. Background Geochemistry of the Bandelier Tuff

The results of geochemical analyses of unaltered and altered samples of the Bandelier Tuff were presented in Appendixes I and II. We have not yet evaluated the data in detail and examined applications to waste management. However, the data show significant variations in both major and trace elements between unaltered and altered samples of the Tuff presumably due to natural alteration processes. Clearly the nature and rates of alteration reactions needs to be defined and potential interactions with radioactive waste elements considered.

## VIII. RECOMMENDATIONS

We have described the stratigraphy of the Bandelier Tuff at selected areas within the Pajarito Plateau and noted the presence of primary and secondary features within the Tuff that probably control hydrologic transport directions. Based on this work, the following recommendations are presented:

1. Field Hydrology Testing. It is critical to determine how primary and secondary features of the Tuff control hydrologic transport rates. A systematic field testing program should be undertaken. This program should first include generic testing to examine the range and magnitude of hydrologic properties for individual cooling units and advance to site specific testing at individual waste disposal pits.

2. Site-Specific Stratigraphic Studies. The stratigraphic procedures we have used should be applied to study of the Bandelier Tuff at major waste disposal sites. These studies are necessary to properly undertake site-specific hydrologic testing.

3. Nevada Test Site Data Base. A wealth of hydrologic data exists at the Nevada Test Site on hydrologic properties of ash-flow tuff. These data have direct application to studies of the Bandelier Tuff.

4. Upgrade Stratigraphic Units in LASL Reports. The existing stratigraphic subdivisions used in LASL reports concerning waste disposal sites needs to be updated. Such an upgrading will have two benefits: (1) It will improve the genetic understanding of defined units. This will allow subsurface projection of units with improved three-dimensional understanding. (2) It will improve the geologic credibility of background geologic information at waste disposal sites. This may be important if the geology of the sites is reviewed by outside agencies.

5. Geochemical Studies. The geochemical study and the results of sample analyses from this work is only partly completed. The work needs to be continued to examine the geochemical potential for radionuclide migration in the Tuff, potential waste-country rock interactions and the possible effects of natural alteration processes on waste stability and migration.

ACKNOWLEDGMENTS

The project benefited considerably from a field conference convened to examine the Bandelier Tuff during April of 1977. Participants included Richard V. Fisher, Hans-Ulrich Schmincke, and Steven Sparks. We are grateful for their lively discussions and insights concerning the geology of the Bandelier Tuff during the week-long conference. Larry Pinkston assisted with the laboratory work.

REFERENCES

1. R. A. Bailey, R. L. Smith, and C. S. Ross, "Stratigraphic Nomenclature of the Volcanic Rocks in the Jemez Mountains," U.S. Geol. Survey Bull. 1274 (1969).

2. E. H. Baltz, J. H. Abrahams, Jr., and W. D. Purtymun, "Preliminary Report on the Geology and Hydrology of Mortandad Canyon near Los Alamos, New Mexico, with Reference to Disposal of Liquid Low-Level Radioactive Waste," U.S. Geol. Survey Open File Report, 105 p (1961).

3. L. M. Brush, "Sediment Sorting in Alluvial Channels," in G. V. Middleton, editor, "Primary Sedimentary Structures and Their Hydrodynamic Interpretation;" Soc. Econ. Paleo. and Min. Spec. Publ., no. 12, p. 25-33 (1965).

4. B. M. Crowe, and R. V. Fisher, "Sedimentary Structures in Base-Surge Deposits with Special Reference to Cross-Bedding, Ubehebe Craters, Death Valley, California," Geol. Soc. Amer. Bull., v. 84, p. 663-682 (1973).

5. W. A. Deer, R. A. Howie, and J. Zussman, "An Introduction to the Rock-Forming Minerals," John Wiley and Sons, Inc. 528 p. (1966).

6. R. R. Doell, G. B. Dalrymple, R. L. Smith, and R. A. Bailey, "Paleomagnetism, Potassium-Argon Ages, and Geology of the Rhyolites and Associated Rocks at the Valles Caldera, New Mexico," Geol. Surv. of Amer. Mem. 116 (1968).

7. J. C. Eichelberger, and F. G. Koch, "Lithic Fragments in the Bandelier Tuff, Jemez Mountains, New Mexico," submitted to J. Volcanol. and Petrol. (1977).

8. R. V. Fisher, "Mechanism of Deposition from Pyroclastic Flows," Amer. Jour. Sci., v. 264, p. 350-363 (1966).

9. R. V. Fisher and A. C. Waters, "Base Surge Bed Forms in Maar Volcanoes," Amer. Jour. Sci., v. 268, p. 157-180 (1969).

10. R. L. Folk, "Petrology of Sedimentary Rocks: Austin, Texas," Hemphill's 159 p (1965).

11. R. L. Griggs, "Geology and Ground-water Resources of the Los Alamos Area, New Mexico," U.S. Geol. Surv. Water-Supply Paper 1753, 107 pp (1964).

12. G. V. Middleton, "Experimental Studies Related to Problems of Flysch Sedimentation," Geol. Assoc. Canada, Spec. Paper No. 7, 253-272 (1970).

13. W. D. Purtymun, "Underground Movement of Tritium from Solid Waste Storage Shafts," Los Alamos Scientific Laboratory Report LA-5286-MS (1973).

14. J. R. Riehle, "Calculated Compaction Profiles of Rhyolitic Ash-Flow Tuffs," *Geol. Soc. Amer. Bull., v. 84, 2193-2216 (1973).*

15. C. S. Ross, R. L. Smith, and R. A. Bailey, "Outline of the Geology of the Jemez Mountains, New Mexico," New Mexico Geological Society 12th Field Conference, *Albuquerque Country* (1961).

16. H. U. Schmincke, R. V. Fisher, and A. C. Waters, "Antidune and Chute and Pool Structures in the Base Surge Deposits of the Laacher See Area, Germany," Sedimentology, v. 20, p. 553-574.

17. M. F. Sheridan, "Fumarolic Mounds and Ridges of the Bishop Tuff, California," Geol. Soc. Amer. Bull., v. 81, 851-868 (1970).

18. M. F. Sheridan, and D. M. Ragan, "Compaction of Ash-Flow Tuffs," in Chilingarian, G. V., and Wolf, K. H., editors, "Compaction of Coarse-Grained Sediments, II: Developments in Sedimentology 18B," Elsevier Publ. Co., Amsterdam, 677-713 (1977).

19. H. T. U. Smith, "Tertiary Geology of the Abiquiu Quadrangle, New Mexico," Jour. Geology, v. 46, no. 7, 933-965 (1938).

20. R. L. Smith, "Zones and Zonal Variations in Welded Ash Flows," U.S. Geol. Surv. Prof. Paper 354-F, 149-159 (1960).

21. R. L. Smith and R. A. Bailey, "The Bandelier Tuff: A Study of Ash-Flow Eruption Cycles from Zoned Magma Chambers," Bull. Volcanol., v. 29, ser. 2, 38-104 (1966).

22. R. L. Smith, R. A. Bailey, and C. S. Ross, "Geologic Map of the Jemez Mountains, New Mexico," U.S. Geological Surv. Misc. Geologic Inv. Map I-571 (1970).

23. M. A. Sommer, "Volatiles $H_2O$, $CO_2$ and CO in Silicate Melt Inclusions in Quartz Phenocrysts from the Rhyolitic Bandelier Air-Fall and Ash-Fall Tuff, New Mexico," Jour. Geol., v. 85, 423-432 (1977).

24. R. S. J. Sparks, "Stratigraphy and Geology of the Ignimbrites of Vulsini Volcano, Central Italy," Geol. Rundschau, v. 64, No. 2 497-523 (1975).

25. R. S. J. Sparks, "Grain-Size Variations in Ignimbrites and Implications for the Transport of Pyroclastic Flows," Sedimentology, v. 23, 147-188 (1976).

26. R. S. J. Sparks, S. Self, and G. P. L. Walker, "Products of Ignimbrite Eruptions," Geology, v. 1, no. 3, 115-118.

27. R. S. J. Sparks, and L. Wilson, "A Model for the Formation of Ignimbrite by Gravitational Column Collapse," Jour. Geol. Soc. of London, v. 132, No. 4, 441-452 (1976).

28. G. A. Taylor, "The 1951 Eruption of Mount Lamington, Papua: Australia," Bur. Mineral. Res. Geol. Geophys. Bull., v. 38, 117 p (1958).

29. G. P. L. Walker, "Grain-Size Characteristics of Pyroclastic Deposits," Jour. Geology, v. 79, 696-714 (1971).

30. M. L. Wheeler, W. J. Smith, and A. F. Gallegos, "A Preliminary Evaluation of the Potential for Plutonium Release from Burial Grounds at Los Alamos Scientific Laboratory," Los Alamos Scientific Laboratory Report LA-6694-MS, 19 p (1977).

31. L. Wilson, "Explosive Volcanic Eruptions - III. Plinian Eruption Columns," Geophys. J. R. Astr. Soc., v. 45, 543-556 (1976).

32. I. J. Winograd, and W. Thordarson, "Hydrogeologic and Hydrochemical Framework, South-Central Great Basin, Nevada-California, with special reference to the Nevada Test Site," U.S. Geological Surv. 712-C, 126 p (1975).

33. R. A. Young, "Water Supply for the Nuclear Rocket Development Station at the U.S. Atomic Energy Commission's Nevada Test Site," U.S. Geol. Surv. Water Supply Paper 1938, 19 p (1972).

APPENDIX I: Partial Chemical Analyses of Selected Samples of Bandelier Tuff
Major Oxides and Chlorine (in Weight Percent).*

| Sample No. | 4250.1 | 4253.3 | 4254.3 | 4257.3 | 4264.1 | 4265.1 | 4265.2 | 4266.1 | 4267.1 | 4267.2 | 4288.1 | 4269.1 | 4269.2 | 4270.1 |
|---|---|---|---|---|---|---|---|---|---|---|---|---|---|---|
| $Al_2O_3$ | 27.21 | 14.78 | 13.96 | 15.12 | 13.81 | 13.51 | 14.04 | 12.17 | 13.91 | 14.15 | 13.26 | 13.57 | 14.98 | 12.98 |
| CaO | 7.56 | 1.37 | 0.60 | 0.56 | 0.57 | <0.5 | <0.5 | 0.52 | 0.44 | <0.5 | 0.28 | 0.76 | 1.18 | 0.27 |
| FeO | 2.44 | 2.26 | 2.30 | 2.16 | 2.33 | 2.92 | 3.09 | 1.29 | 2.37 | 3.04 | 2.78 | 2.65 | 2.75 | 2.02 |
| MgO | 3.20 | <0.5 | <0.5 | <0.5 | <0.5 | <0.5 | <0.5 | <0.5 | <0.5 | <0.5 | <0.5 | <0.5 | <0.5 | <0.5 |
| $Na_2O$ | 0.43 | 5.66 | 4.74 | 4.52 | 4.54 | 4.61 | 4.72 | 3.98 | 4.66 | 4.88 | 4.38 | 4.49 | 4.91 | 4.35 |
| $K_2O$ | 3.41 | 3.19 | 3.64 | 3.24 | 3.42 | 3.41 | 3.35 | 3.48 | 3.83 | 3.55 | 3.38 | 3.61 | 4.00 | 4.05 |
| $TiO_2$ | 1.02 | <0.03 | <0.03 | 0.22 | <0.03 | <0.03 | <0.03 | <0.03 | 0.04 | <0.03 | <0.03 | <0.03 | <0.03 | <0.03 |
| MnO | 0.07 | 0.09 | 0.07 | 0.06 | 0.09 | 0.08 | 0.09 | 0.07 | 0.08 | 0.09 | 0.08 | 0.08 | 0.10 | 0.07 |
| Cl | <0.02 | 0.79 | 0.25 | 0.08 | 0.27 | 0.19 | 0.21 | 0.16 | 0.17 | 0.26 | 0.19 | 0.18 | 0.84 | 0.11 |

4250.1 - channel sample, basal unwelded zone, cooling unit 1 (CU 1)**
4253.3 - channel sample, zone of partial welding, CU 1
4254.3 - channel sample, upper unwelded zone, CU 1
4257.3 - channel sample, the ash flow sequence, the Otowi Member
4264.1 - representative sample from base, CU 1
4265.1 - representative sample 1.8 m from base, CU 1
4265.2 - PUmice sample 1.8 m from base, CU 1
4266.1 - representative sample 3.7 m from base of CU 1
4267.1 - representative sample 5.5 m from base of CU 1
4267.2 - Pumice sample 5.5 m from base of CU 1
4268.1 - representative sample 7.4 m from base of CU 1
4269.1 - representative sample 9.2 m from base of CU 1
4269.2 - Pumice sample 9.2 m from base of CU 1
4270.1 - representative sample 11.1 m from base of CU 1

* Analyses by neutron activation. Analyst M. E. Bunker.
** Listed samples from composite column one.

APPENDIX I (Cont'd.)

| Sample No. | 4271.3 | 4272.1 | 4274.1 | 4276.1 | 4277.1 | 4280.1 | 4281.1 | 4282.1 | 4283.1 | 4284.1 | 4285.1 | 4291.1 |
|---|---|---|---|---|---|---|---|---|---|---|---|---|
| $Al_2O_3$ | 14.85 | 14.62 | 12.28 | 14.51 | 13.30 | 12.93 | 13.25 | 12.94 | 14.59 | 14.11 | 13.94 | 13.47 |
| CaO | <0.5 | 1.46 | 1.25 | <0.5 | <0.5 | 0.46 | 0.34 | <0.5 | <0.5 | <0.5 | 0.46 | <0.5 |
| FeO | 2.01 | 2.02 | 2.15 | 1.76 | 2.12 | 1.85 | 0.87 | 1.69 | 1.84 | 2.06 | 1.83 | 1.99 |
| MgO | <0.5 | <0.5 | <0.5 | <0.5 | <0.5 | <0.5 | <0.5 | <0.5 | <0.5 | <0.5 | <0.5 | <0.5 |
| $Na_2O$ | 4.54 | 5.14 | 4.19 | 4.88 | 4.66 | 4.39 | 4.64 | 4.29 | 4.33 | 4.49 | 4.53 | 4.54 |
| $K_2O$ | 4.17 | 3.17 | 3.41 | 3.55 | 3.45 | 3.24 | 3.79 | 3.28 | 3.85 | 3.65 | 4.10 | 3.96 |
| $TiO_2$ | <0.03 | <0.03 | <0.03 | 0.07 | 0.05 | 0.06 | <0.03 | <0.03 | <0.03 | <0.03 | 0.14 | 0.11 |
| MnO | 0.09 | 0.08 | 0.07 | 0.08 | 0.07 | 0.07 | 0.06 | 0.06 | 0.06 | 0.07 | 0.06 | 0.06 |
| Cl | <0.03 | 0.24 | 0.12 | 0.10 | <0.02 | <0.02 | 0.03 | <0.02 | <0.02 | <0.02 | <0.02 | <0.02 |

4371.3 - representative sample 11.9 m from base of CU 1*
4272.1 - representative sample from base, zone of partial welding of CU 1
4274.1 - representative sample 3.6 m from base of zone of partial welding of CU 1
4276.1 - representative sample from top of zone of partial welding of CU 1 (8.6 m from base of zone)
4277.3 - channel sample of CU 2
4280.1 - representative sample from base of CU 2
4281.1 - representative sample 9.2 m from base of CU 2
4282.1 - representative sample 12.5 m from base of CU 2
4283.1 - representative sample 14.1 m from base of CU 2
4284.1 - representative sample 15.8 m from base of CU 2
4285.1 - representative sample 17.4 m from base of CU 2
4291.1 - representative sample from zone of partial welding of CU 3

*Listed sample from composite column one.

APPENDIX I (Cont'd.)

| Sample No. | 4317.3 | 4318.3 | 4319.3 | 4323.3 | 4324.3 | 4325.3 | 4326.3 | 4327.3 | 4328.3 | 4329.3 | 4330.3 | 4331.3 |
|---|---|---|---|---|---|---|---|---|---|---|---|---|
| $Al_2O_3$ | 14.04 | 14.55 | 12.13 | 10.68 | 14.15 | 13.26 | 5.22 | 13.62 | 13.64 | 14.25 | 11.45 | 13.77 |
| CaO | 0.56 | <0.04 | <0.04 | 0.17 | 1.05 | 2.90 | <0.04 | <0.04 | <0.04 | 0.61 | 0.44 | <0.04 |
| FeO | 1.69 | 1.65 | 1.66 | 1.85 | 2.02 | 1.39 | 2.03 | 1.85 | 2.41 | 2.60 | 2.23 | 1.73 |
| MgO | <0.30 | <0.30 | <0.30 | <0.30 | <0.30 | 1.20 | <0.30 | <0.30 | <0.30 | <0.30 | <0.30 | <0.30 |
| $Na_2O$ | 4.73 | 4.70 | 3.98 | 3.30 | 4.08 | 2.93 | 4.74 | 4.73 | 4.74 | 4.72 | 3.77 | 4.74 |
| $K_2O$ | 3.08 | 3.16 | 3.30 | 2.94 | 3.20 | 1.94 | 3.29 | 3.36 | 3.32 | 2.96 | 3.51 | 3.34 |
| $TiO_2$ | <0.02 | 0.14 | 0.09 | <0.02 | 0.14 | 0.10 | <0.02 | <0.02 | <0.02 | <0.02 | <0.02 | <0.02 |
| MnO | 0.07 | 0.08 | 0.07 | 0.06 | 0.07 | 0.08 | 0.06 | 0.09 | 0.09 | 0.09 | 0.07 | 0.08 |
| Cl | 0.08 | <0.02 | 0.14 | 0.14 | 0.06 | <0.02 | 0.17 | 0.20 | 0.20 | 0.28 | 0.18 | 0.26 |

4317.3 - channel sample, CU 3*
4318.3 - channel sample, CU 2
4319.3 - channel sample, CU 1
4323.3 - channel sample, ash-flow sequence of Otowi Member
4324.3 - channel sample of Guaje Pumice Bed
4325.3 - upper paleo-aquifer ledge, Ancho Canyon
4326.3 - increment sample 0-10 cm above upper paleo-aquifer ledge, Ancho Canyon
4327.3 - increment sample 10-20 cm above upper paleo-aquifer ledge, Ancho Canyon
4328.3 - increment sample 20-30 cm above upper paleo-aquifer ledge, Ancho Canyon
4329.3 - increment sample 30-40 cm above upper paleo-aquifer ledge, Ancho Canyon
4330.3 - increment sample 40-50 cm above upper paleo-aquifer ledge, Ancho Canyon
4331.3 - increment sample 50-60 cm above upper paleo-aquifer ledge, Ancho Canyon

*Listed samples from composite column three.

APPENDIX I (Cont'd.)

| Sample No. | 4332.3 | 4333.3 | 4334.3 | 4335.3 | 4336.3 | 4337.3 | 4338.3 | 4339.3 | 4340.3 | 4341.3 | 4342.3 | 4343.3 |
|---|---|---|---|---|---|---|---|---|---|---|---|---|
| $Al_2O_3$ | 13.98 | 12.45 | 12.22 | 12.64 | 14.79 | 12.00 | 11.30 | 12.04 | 14.13 | -- | 12.87 | 11.70 |
| CaO | 0.72 | 0.28 | 0.37 | <0.05 | 1.40 | 0.58 | 1.57 | 0.85 | 0.64 | -- | <0.05 | 1.35 |
| FeO | 2.10 | 2.17 | 1.79 | 1.56 | 1.87 | 1.53 | 1.57 | 1.70 | 1.79 | 1.89 | 1.96 | 1.84 |
| MgO | <0.03 | <0.03 | <0.03 | <0.03 | 0.83 | <0.03 | <0.03 | <0.03 | <0.03 | -- | <0.03 | <0.03 |
| $Na_2O$ | 4.68 | 4.15 | 4.07 | 4.11 | 3.40 | 3.49 | 2.10 | 3.38 | 4.22 | -- | 3.73 | 3.45 |
| $K_2O$ | 2.95 | 2.99 | 2.41 | 3.47 | 3.20 | 3.71 | 2.77 | 4.16 | 4.08 | 4.05 | 4.42 | 4.08 |
| $TiO_2$ | <0.02 | <0.02 | <0.02 | <0.02 | <0.02 | <0.02 | <0.02 | <0.02 | <0.02 | -- | 0.10 | <0.02 |
| MnO | 0.09 | 0.08 | 0.07 | 0.07 | 0.09 | 0.07 | 0.07 | 0.07 | 0.08 | -- | 0.08 | 0.07 |
| Cl | 0.30 | 0.14 | 0.15 | 0.14 | 0.13 | 0.10 | 0.40 | 0.11 | 0.17 | -- | 0.15 | 0.15 |

4332.3 - increment sample 60-70 cm above upper paleo-aquifer ledge, Ancho Canyon*
4333.3 - increment sample 70-80 cm above upper paleo-aquifer ledge, Ancho Canyon
4334.3 - increment sample 80-90 cm above upper paleo-aquifer ledge, Ancho Canyon
4335.3 - increment sample 90-100 cm above upper paleo-aquifer ledge, Ancho Canyon
4336.3 - second paleo-aquifer ledge (from upper ledge), Ancho Canyon
4337.3 - third paleo-aquifer ledge (from upper ledge), Ancho Canyon
4338.3 - fourth paleo-aquifer ledge (from upper ledge), Ancho Canyon
4339.3 - fifth paleo-aquifer ledge (from upper ledge), Ancho Canyon
4340.3 - channel sample of rock between fifth and fourth ledges, Ancho Canyon
4341.3 - channel sample of rock between fourth and third ledges, Ancho Canyon
4342.3 - channel sample of rock between third and second ledges, Ancho Canyon
4343.3 - channel sample of rock between second and upper ledges, Ancho Canyon

*Listed samples from composite column three.

APPENDIX II: Partial Chemical Analyses of Selected Samples of Bandelier Tuff
Trace Elements (in ppm).*

| Sample No. | 4250.1 | 4253.3 | 4254.3 | 4257.3 | 4264.1 | 4265.1 | 4265.2 | 4266.1 | 4267.1 | 4267.2 | 4268.1 | 4269.1 | 4269.2 | 4270.1 |
|---|---|---|---|---|---|---|---|---|---|---|---|---|---|---|
| Sb | <1.0 | 1.3 | 1.4 | <1.0 | 1.4 | 1.7 | 1.8 | <1.0 | 1.2 | 1.9 | 1.9 | 1.9 | 1.8 | 1.7 |
| As | <20.0 | <20.0 | <20.0 | <20.0 | <20.0 | <20.0 | <20.0 | <20.0 | <20.0 | <20.0 | <20.0 | <20.0 | <20.0 | <20.0 |
| Ba | 2630.0 | <400.0 | <400.0 | 304.0 | <400.0 | <400.0 | <400.0 | <400.0 | <400.0 | <400.0 | <400.0 | <400.0 | <400.0 | <400.0 |
| Br | <5.0 | <5.0 | <5.0 | <5.0 | <5.0 | <5.0 | <5.0 | <5.0 | <5.0 | <5.0 | <5.0 | <5.0 | <5.0 | <5.0 |
| Cs | 7.2 | 6.6 | 3.7 | 4.2 | 7.7 | 7.3 | 9.7 | 6.3 | 6.9 | 7.5 | 8.1 | 8.4 | 10.5 | 12.4 |
| Ce | 105.0 | 103.0 | 104.0 | 80.6 | 120.0 | 107.0 | 119.0 | 93.6 | 104.0 | 110.0 | 99.1 | 118.0 | 90.0 | 103.0 |
| Cr | 10.2 | 9.9 | 9.4 | 8.3 | 5.4 | 11.8 | 16.2 | 17.3 | 11.8 | 13.7 | 13.3 | 11.8 | 14.3 | 12.9 |
| Co | 1.4 | 1.4 | 1.5 | 1.4 | 0.9 | 33.4 | 1.0 | 1.7 | 62.6 | 1.7 | 1.8 | 20.2 | 21.9 | 1.3 |
| Cu | <80.0 | <80.0 | <80.0 | <80.0 | <80.0 | <80.0 | <80.0 | <80.0 | <80.0 | <80.0 | <80.0 | <80.0 | <80.0 | <80.0 |
| Dy | 11.4 | 10.4 | 9.8 | 6.8 | 15.1 | 13.6 | 15.1 | 10.8 | 12.1 | 16.0 | 12.2 | 15.6 | 19.6 | 11.9 |
| Eu | 0.5 | 0.5 | 0.5 | 0.4 | 0.7 | 0.5 | 0.5 | 0.5 | 0.5 | 0.5 | 0.5 | 0.5 | 0.5 | 0.5 |
| Ga | <20.0 | <20.0 | 20.3 | 20.1 | <20.0 | <20.0 | <20.0 | <20.0 | <20.0 | 35.1 | 22.7 | <20.0 | <20.0 | <20.0 |
| Au | <0.1 | <0.1 | <0.1 | <0.1 | <0.1 | <0.1 | <0.1 | <0.1 | <0.1 | <0.1 | <0.1 | <0.1 | <0.1 | <0.1 |
| Hf | 10.0 | 9.6 | 9.5 | 7.8 | 13.7 | 11.2 | 13.4 | 10.5 | 10.0 | 11.8 | 10.6 | 9.2 | 12.3 | 9.6 |
| La | 42.7 | 41.8 | 38.2 | 40.4 | 46.0 | 40.5 | 47.4 | 40.2 | 40.8 | 40.1 | 40.7 | 37.7 | 43.2 | 39.2 |
| Lu | 1.2 | 1.0 | 1.1 | 0.7 | 1.5 | 1.2 | 1.6 | 1.2 | 1.1 | 1.4 | 1.3 | 1.0 | 1.4 | 1.1 |
| Hg | <4.0 | <4.0 | <4.0 | <4.0 | <4.0 | <4.0 | <4.0 | <4.0 | <4.0 | <4.0 | <4.0 | <4.0 | <4.0 | <4.0 |
| Rb | 219.0 | 211.0 | 212.0 | 149.0 | 293.0 | 221.0 | 266.0 | 201.0 | 204.0 | 273.0 | 232.0 | 195.0 | 254.0 | 217.0 |
| Sm | 8.4 | 8.6 | 9.5 | 6.3 | 10.6 | 9.3 | 9.5 | 8.2 | 9.2 | 9.9 | 8.5 | 8.7 | 11.1 | 8.9 |
| Sc | 1.2 | 1.0 | 1.0 | 2.0 | 1.1 | 1.1 | 0.8 | 1.5 | 1.0 | 0.8 | 1.0 | 1.0 | 0.8 | 0.9 |
| Ag | <5.0 | <5.0 | <5.0 | <5.0 | <5.0 | <5.0 | <5.0 | <5.0 | <5.0 | <5.0 | <5.0 | <5.0 | <5.0 | <5.0 |
| Sr | <300.0 | <300.0 | <300.0 | <300.0 | <300.0 | <300.0 | <300.0 | <300.0 | <300.0 | <300.0 | <300.0 | <300.0 | <300.0 | <300.0 |
| Ta | 6.2 | 5.9 | 5.2 | 4.8 | 9.7 | 9.1 | 10.1 | 7.1 | 1.1 | 7.4 | 7.9 | 7.0 | 9.3 | 6.3 |
| Tb | 3.0 | 3.5 | 3.0 | 2.5 | 4.3 | 4.0 | 4.6 | 2.8 | 4.3 | 4.1 | 4.2 | 3.3 | 3.8 | 1.1 |
| Th | 27.3 | 25.4 | 23.7 | 21.9 | 36.4 | 30.1 | 36.2 | 26.6 | 28.4 | 32.5 | 28.8 | 25.0 | 32.3 | 26.0 |
| U | 4.41 | 7.67 | 7.36 | 6.86 | 11.35 | 9.38 | 11.23 | 8.45 | 8.85 | 10.61 | 9.04 | 8.08 | 10.31 | 8.24 |
| V | 253.0 | <5.0 | <5.0 | 8.9 | <5.0 | <5.0 | <5.0 | <5.0 | <5.0 | <5.0 | <5.0 | 6.4 | <5.0 | <5.0 |
| W | <5.0 | <5.0 | <5.0 | <5.0 | <5.0 | 53.4 | <5.0 | 22.1 | 115.0 | <5.0 | 27.3 | 38.5 | 35.3 | <5.0 |
| Yb | 8.2 | 7.8 | 7.6 | 4.2 | 10.9 | 8.9 | 11.4 | 7.7 | 9.6 | 10.1 | 9.0 | 7.2 | 9.7 | 7.8 |
| Zn | 131.0 | 128.0 | 104.0 | 97.0 | 144.0 | 116.0 | 152.0 | 124.0 | 119.0 | 142.0 | 106.0 | 98.7 | 135.0 | 107.0 |

*Analyses by neutron activation except for uranium which is by delayed neutron counting. Analyst M. E. Bunker.

APPENDIX II (Cont'd.)

| Sample No. | 4271.3 | 4272.1 | 4274.1 | 4276.1 | 4277.1 | 4280.1 | 4281.1 | 4282.1 | 4283.1 | 4284.1 | 4285.1 | 4291.1 |
|---|---|---|---|---|---|---|---|---|---|---|---|---|
| Sb | 1.4 | 0.9 | 1.1 | <1.0 | <1.0 | <1.0 | <1.0 | <1.0 | <1.0 | <1.0 | <1.0 | <1.0 |
| As | <20.0 | <20.0 | <20.0 | <20.0 | <20.0 | <20.0 | <20.0 | <20.0 | <20.0 | <20.0 | <20.0 | <20.0 |
| Ba | <400.0 | <400.0 | <400.0 | <400.0 | <400.0 | <400.0 | <400.0 | <400.0 | <400.0 | <400.0 | <400.0 | <400.0 |
| Br | <5.0 | <5.0 | <5.0 | <5.0 | <5.0 | <5.0 | <5.0 | <5.0 | <5.0 | <5.0 | <5.0 | <5.0 |
| Cs | 8.0 | 6.2 | 5.3 | 4.6 | 2.2 | 3.3 | 2.8 | 2.7 | 2.5 | 2.3 | 2.9 | 1.8 |
| Ce | 118.0 | 120.0 | 120.0 | 99.8 | 99.3 | 96.8 | 102.0 | 94.1 | 97.7 | 91.4 | 102.0 | 108.0 |
| Cr | 12.2 | 20.4 | 12.5 | 9.9 | 18.5 | 9.5 | 9.2 | <15.0 | 9.6 | 15.8 | 5.5 | 10.4 |
| Co | 49.3 | 1.3 | 81.0 | 38.3 | 1.2 | 1.2 | 168.0 | 103.0 | 1.3 | 86.2 | 86.6 | 23.4 |
| Cu | <80.0 | <80.0 | <80.0 | <80.0 | <80.0 | <80.0 | <80.0 | <80.0 | <80.0 | <80.0 | <80.0 | <80.0 |
| Dy | 15.8 | 13.8 | 10.7 | 14.5 | 6.6 | 9.6 | 6.9 | 6.7 | 6.6 | 9.7 | 9.2 | 6.3 |
| Eu | 0.6 | 0.5 | 0.4 | 0.5 | 0.3 | 0.4 | 0.4 | 0.3 | 0.4 | 0.4 | 0.4 | 0.4 |
| Ga | <20.0 | <20.0 | 20.9 | <20.0 | 29.4 | <20.0 | <20.0 | <20.0 | <20.0 | 23.3 | <20.0 | 22.1 |
| Au | <0.1 | <0.1 | <0.1 | <0.1 | <0.1 | <0.1 | <0.1 | <0.1 | <0.1 | <0.1 | <0.1 | <0.1 |
| Hf | 10.1 | 10.0 | 10.7 | 10.5 | 7.7 | 7.7 | 7.5 | 7.7 | 7.3 | 7.4 | 8.0 | 8.1 |
| La | 47.5 | 54.7 | 59.6 | 55.4 | 48.9 | 52.2 | 52.8 | 50.6 | 48.7 | 56.0 | 51.5 | 58.0 |
| Lu | 1.3 | 1.3 | 1.3 | 1.2 | 0.8 | 0.8 | 0.8 | 0.7 | 0.8 | 0.8 | 0.7 | 0.7 |
| Hg | <4.0 | <4.0 | <4.0 | <4.0 | <4.0 | <4.0 | <4.0 | <4.0 | <4.0 | <4.0 | <4.0 | < 4.0 |
| Rb | 233.0 | 201.0 | 215.0 | 220.0 | 129.0 | 142.0 | 161.0 | 136.0 | 129.0 | 118.0 | 119.0 | 114.0 |
| Sm | 11.9 | 13.6 | 16.0 | 11.7 | 7.8 | 8.4 | 8.2 | 7.9 | 8.2 | 7.6 | 7.6 | 8.1 |
| Sc | 1.1 | 1.1 | 1.1 | 1.0 | 1.2 | 1.4 | 1.2 | 1.3 | 1.3 | 1.4 | 1.5 | 1.6 |
| Ag | <5.0 | <5.0 | <5.0 | <5.0 | <5.0 | <5.0 | <5.0 | <5.0 | <5.0 | <5.0 | <5.0 | <5.0 |
| Sr | <300.0 | <300.0 | <300.0 | <300.0 | <300.0 | <300.0 | <300.0 | <300.0 | <300.0 | <300.0 | <300.0 | <300.0 |
| Ta | 9.2 | 7.0 | 8.4 | 7.8 | 4.2 | 3.7 | 9.2 | 6.6 | 3.2 | 7.9 | 7.1 | 4.9 |
| Tb | 1.5 | 1.1 | 1.4 | 1.2 | 0.9 | 0.8 | 0.9 | 1.1 | 0.7 | 1.0 | 0.8 | 0.9 |
| Th | 29.5 | 29.2 | 28.2 | 27.1 | 18.4 | 17.9 | 17.9 | 16.2 | 16.8 | 16.3 | 15.1 | 16.4 |
| U | 8.2 | 7.6 | 7.8 | 8.1 | 4.6 | 4.9 | 4.5 | 4.4 | 4.4 | 4.0 | 4.1 | 8.1 |
| V | <5.0 | 4.5 | <5.0 | <5.0 | 7.0 | 5.7 | <5.0 | <5.0 | <5.0 | <5.0 | <5.0 | 5.0 |
| W | 86.5 | 5.0 | 105.0 | 59.7 | 5.0 | 5.0 | 269.0 | 158.0 | 5.0 | 131.0 | 147.0 | 44.0 |
| Tb | 9.7 | 10.1 | 9.4 | 9.3 | 5.3 | 5.5 | 5.6 | 5.0 | 5.3 | 5.5 | 5.3 | 4.9 |
| Zn | 123.0 | 127.0 | 119.0 | 120.0 | 97.3 | 88.9 | 98.6 | 108.0 | 79.4 | 115.0 | 98.2 | 91.2 |

APPENDIX II (Cont'd.)

| Sample No. | 4271.3 | 4272.1 | 4274.1 | 4276.1 | 4277.1 | 4280.1 | 4281.1 | 4282.1 | 4283.1 | 4284.1 | 4285.1 | 4291.1 |
|---|---|---|---|---|---|---|---|---|---|---|---|---|
| Sb | 1.4 | 0.9 | 1.1 | <1.0 | <1.0 | <1.0 | <1.0 | <1.0 | <1.0 | <1.0 | <1.0 | <1.0 |
| As | <20.0 | <20.0 | <20.0 | <20.0 | <20.0 | <20.0 | <20.0 | <20.0 | <20.0 | <20.0 | <20.0 | <20.0 |
| Ba | <400.0 | <400.0 | <400.0 | <400.0 | <400.0 | <400.0 | <400.0 | <400.0 | <400.0 | <400.0 | <400.0 | <400.0 |
| Br | <5.0 | <5.0 | <5.0 | <5.0 | <5.0 | <5.0 | <5.0 | <5.0 | <5.0 | <5.0 | <5.0 | <5.0 |
| Cs | 8.0 | 6.2 | 5.3 | 4.6 | 2.2 | 3.3 | 2.8 | 2.7 | 2.5 | 2.3 | 2.9 | 1.8 |
| Ce | 118.0 | 120.0 | 120.0 | 99.8 | 99.3 | 96.8 | 102.0 | 94.1 | 97.7 | 91.4 | 102.0 | 108.0 |
| Cr | 12.2 | 20.4 | 12.5 | 9.9 | 18.5 | 9.5 | 9.2 | <15.0 | 9.6 | 15.8 | 5.5 | 10.4 |
| Co | 49.3 | 1.3 | 81.0 | 38.3 | 1.2 | 1.2 | 168.0 | 103.0 | 1.3 | 86.2 | 86.6 | 23.4 |
| Cu | <80.0 | <80.0 | <80.0 | <80.0 | <80.0 | <80.0 | <80.0 | <80.0 | <80.0 | <80.0 | <80.0 | <80.0 |
| Dy | 15.8 | 13.8 | 10.7 | 14.5 | 6.6 | 9.6 | 6.9 | 6.7 | 6.6 | 9.7 | 9.2 | 6.3 |
| Eu | 0.6 | 0.5 | 0.4 | 0.5 | 0.3 | 0.4 | 0.4 | 0.3 | 0.4 | 0.4 | 0.4 | 0.4 |
| Ga | <20.0 | <20.0 | 20.9 | <20.0 | 29.4 | <20.0 | <20.0 | <20.0 | <20.0 | 23.3 | <20.0 | 22.1 |
| Au | <0.1 | <0.1 | <0.1 | <0.1 | <0.1 | <0.1 | <0.1 | <0.1 | <0.1 | <0.1 | <0.1 | <0.1 |
| Hf | 10.1 | 10.0 | 10.7 | 10.5 | 7.7 | 7.7 | 7.5 | 7.7 | 7.3 | 7.4 | 8.0 | 8.1 |
| La | 47.5 | 54.7 | 59.6 | 55.4 | 48.9 | 52.2 | 52.8 | 50.6 | 48.7 | 56.0 | 51.5 | 58.0 |
| Lu | 1.3 | 1.3 | 1.3 | 1.2 | 0.8 | 0.8 | 0.8 | 0.7 | 0.8 | 0.8 | 0.7 | 0.7 |
| Hg | <4.0 | <4.0 | <4.0 | <4.0 | <4.0 | <4.0 | <4.0 | <4.0 | <4.0 | <4.0 | <4.0 | < 4.0 |
| Rb | 233.0 | 201.0 | 215.0 | 220.0 | 129.0 | 142.0 | 161.0 | 136.0 | 129.0 | 118.0 | 119.0 | 114.0 |
| Sm | 11.9 | 13.6 | 16.0 | 11.7 | 7.8 | 8.4 | 8.2 | 7.9 | 8.2 | 7.6 | 7.6 | 8.1 |
| Sc | 1.1 | 1.1 | 1.1 | 1.0 | 1.2 | 1.4 | 1.2 | 1.3 | 1.3 | 1.4 | 1.5 | 1.6 |
| Ag | <5.0 | <5.0 | <5.0 | <5.0 | <5.0 | <5.0 | <5.0 | <5.0 | <5.0 | <5.0 | <5.0 | <5.0 |
| Sr | <300.0 | <300.0 | <300.0 | <300.0 | <300.0 | <300.0 | <300.0 | <300.0 | <300.0 | <300.0 | <300.0 | <300.0 |
| Ta | 9.2 | 7.0 | 8.4 | 7.8 | 4.2 | 3.7 | 9.2 | 6.6 | 3.2 | 7.9 | 7.1 | 4.9 |
| Tb | 1.5 | 1.1 | 1.4 | 1.2 | 0.9 | 0.8 | 0.9 | 1.1 | 0.7 | 1.0 | 0.8 | 0.9 |
| Th | 29.5 | 29.2 | 28.2 | 27.1 | 18.4 | 17.9 | 17.9 | 16.2 | 16.8 | 16.3 | 15.1 | 16.4 |
| U | 8.2 | 7.6 | 7.8 | 8.1 | 4.6 | 4.9 | 4.5 | 4.4 | 4.4 | 4.0 | 4.1 | 8.1 |
| V | <5.0 | 4.5 | <5.0 | <5.0 | 7.0 | 5.7 | <5.0 | <5.0 | <5.0 | <5.0 | <5.0 | 5.0 |
| W | 86.5 | 5.0 | 105.0 | 59.7 | 5.0 | 5.0 | 269.0 | 158.0 | 5.0 | 131.0 | 147.0 | 44.0 |
| Tb | 9.7 | 10.1 | 9.4 | 9.3 | 5.3 | 5.5 | 5.6 | 5.0 | 5.3 | 5.5 | 5.3 | 4.9 |
| Zn | 123.0 | 127.0 | 119.0 | 120.0 | 97.3 | 88.9 | 98.6 | 108.0 | 79.4 | 115.0 | 98.2 | 91.2 |

APPENDIX II (Cont'd.)

| Sample No. | 4332.3 | 4333.3 | 4334.3 | 4335.3 | 4336.3 | 4337.3 | 4338.3 | 4339.3 | 4340.3 | 4341.3 | 4342.3 | 4343.3 |
|---|---|---|---|---|---|---|---|---|---|---|---|---|
| Sb | 0.6 | 0.6 | <1.0 | <1.0 | <1.0 | <1.0 | 0.3 | 0.5 | 0.9 | 0.7 | <1.0 | 0.6 |
| As | <20.0 | <20.0 | <20.0 | 5.2 | <20.0 | <20.0 | <20.0 | <20.0 | <20.0 | <20.0 | <20.0 | <20.0 |
| Ba | <400.0 | <400.0 | <400.0 | <400.0 | <400.0 | <400.0 | <400.0 | <400.0 | <400.0 | <400.0 | <400.0 | <400.0 |
| Br | <5.0 | <5.0 | <5.0 | <5.0 | <5.0 | <5.0 | <5.0 | <5.0 | <5.0 | <5.0 | <5.0 | <5.0 |
| Cs | 6.6 | 5.5 | 5.7 | 6.6 | 6.3 | 5.3 | 3.9 | 5.8 | 6.3 | 5.7 | 4.7 | 5.8 |
| Ce | 98.8 | 95.6 | 94.2 | 91.3 | 125.0 | 91.4 | 78.7 | 88.9 | 97.7 | 97.6 | 98.7 | 90.2 |
| Cr | 9.6 | 14.1 | 12.7 | 4.8 | 8.8 | 6.2 | 8.5 | 1.1 | 6.8 | 13.1 | 10.1 | 11.6 |
| Co | 25.5 | 1.5 | 41.3 | 130.0 | 26.5 | 43.8 | 1.5 | 15.6 | 39.9 | 24.1 | 44.2 | 1.4 |
| Cu | <80.0 | <80.0 | <80.0 | <80.0 | <80.0 | <80.0 | <80.0 | <80.0 | 278.0 | ---- | <80.0 | <80.0 |
| Dy | 12.1 | 10.6 | 11.3 | 11.8 | 15.2 | 12.4 | 9.6 | 12.2 | 20.6 | ---- | 13.7 | 11.4 |
| Eu | 0.4 | 0.5 | 0.4 | <0.5 | <0.5 | 0.5 | 0.4 | 0.5 | <0.5 | <0.5 | <0.5 | 0.3 |
| Ga | <20.0 | <20.0 | <20.0 | <20.0 | 26.0 | <20.0 | 20.7 | <20.0 | <20.0 | <20.0 | <20.0 | 36.6 |
| Au | <0.1 | <0.1 | <0.1 | <0.1 | <0.1 | <0.1 | <0.1 | <0.1 | <0.1 | <0.1 | <0.1 | <0.1 |
| Hf | 10.2 | 9.7 | 9.7 | 10.9 | 10.7 | 9.8 | 9.7 | 9.7 | 10.1 | 10.6 | 10.4 | 9.4 |
| La | 32.4 | 32.8 | 32.9 | 32.1 | 33.8 | 30.0 | 29.7 | 30.6 | 31.1 | 33.1 | 30.7 | 29.2 |
| Lu | 1.0 | 1.0 | 1.0 | 1.1 | 1.2 | 1.1 | 1.1 | 1.0 | 1.1 | 1.2 | 1.2 | 1.1 |
| Hg | <5.0 | <5.0 | <5.0 | <5.0 | <5.0 | <5.0 | <5.0 | <5.0 | <5.0 | <5.0 | <5.0 | <5.0 |
| Rb | 225.0 | 193.0 | 216.0 | 216.0 | 186.0 | 188.0 | 134.0 | 201.0 | 249.0 | 232.0 | 221.0 | 167.0 |
| Sm | 6.7 | 7.0 | 6.9 | 7.4 | 4.8 | 6.7 | 6.4 | 6.4 | 6.6 | 7.2 | 7.0 | 6.1 |
| Sc | 1.4 | 1.0 | 1.0 | 1.2 | 1.0 | 1.0 | 0.9 | 1.0 | 1.0 | 1.0 | 1.0 | 1.0 |
| Ag | <5.0 | <5.0 | <5.0 | <5.0 | <5.0 | <5.0 | <5.0 | <5.0 | <5.0 | <5.0 | <5.0 | <5.0 |
| Sr | <300.0 | <300.0 | <300.0 | <300.0 | <300.0 | <300.0 | 835.0 | <300.0 | <300.0 | ---- | <300.0 | <300.0 |
| Ta | 7.7 | 6.9 | 8.4 | 13.6 | 8.6 | 7.7 | 6.5 | 7.0 | 8.6 | 7.3 | 8.9 | 5.6 |
| Tb | 1.2 | 1.1 | 0.9 | 1.7 | 1.2 | 1.3 | 1.3 | 1.0 | 0.8 | 1.1 | 1.2 | 1.1 |
| Th | 24.6 | 26.7 | 25.5 | 26.0 | 28.7 | 24.3 | 25.2 | 26.0 | 25.9 | 27.3 | 25.9 | 24.4 |
| U | 8.43 | 8.99 | 8.69 | 8.98 | 8.76 | 8.64 | 7.81 | 9.03 | 8.93 | 9.33 | 9.02 | 8.36 |
| V | 12.7 | <5.0 | <5.0 | <5.0 | <5.0 | <5.0 | 6.9 | 7.7 | <5.0 | ---- | <5.0 | <5.0 |
| W | 42.3 | <5.0 | 77.9 | 248.0 | 50.6 | 87.9 | <5.0 | 33.0 | 80.1 | 45.9 | 86.9 | 4.5 |
| Tb | 1.2 | 1.1 | 0.9 | 1.7 | 1.2 | 1.3 | 1.3 | 1.0 | 0.8 | 1.1 | 1.2 | 1.1 |
| Zn | 145.0 | 143.0 | 137.0 | 141.0 | 190.0 | 144.0 | 127.0 | 128.0 | 124.0 | 133.0 | 120.0 | 112.0 |

APPENDIX III: Analytic detection limits for the elements analyzed by neutron activation and uranium by delayed neutron counting (all values in ppm). S=short count, I=intermediate count and L=long count spectra.

| | | | | | | | | |
|---|---|---|---|---|---|---|---|---|
| Al | 200 | S | Eu | 0.8 | L | Sc | 0.1 | L |
| Sb | 1 | L | Ga | 20 | I | Ag | 5 | L |
| As | 20 | I | Au | 0.1 | L | Na | 150 | S |
| Ba | 400 | S | Hf | 3 | L | Sr | 300 | S |
| Br | 5 | I | Fe | 2000 | L | Ta | 1 | L |
| Ca | 5000 | S | La | 6 | L | Tb | 2 | L |
| Cs | 2 | L | Lu | 0.3 | L | Th | 2 | L |
| Ce | 20 | L | Mg | 3000 | S | Ti | 200 | S |
| Cl | 200 | S | Mn | 10 | S | U | $2 \times 10^{-5}$ | - |
| Cr | 20 | L | Hg | 5 | L | V | 5 | S |
| Co | 2 | L | K | 5000 | I | W | 5 | I |
| Cu | 80 | S | Rb | 30 | L | Yb | 3 | L |
| Dy | 2 | S | Sm | 0.5 | L | Zn | 50 | L |

APPENDIX III (Cont'd.)

| | | | | |
|---|---|---|---|---|
| 77.04236.2 | core | 1.7 | 55.5 | 42.8 |
| | rim | 1.8 | 57.9 | 40.4 |
| | core | 1.3 | 53.0 | 45.7 |
| | rim | 2.3 | 58.4 | 39.31 |
| 77.04240.2 | | | | |
| | core | 1.0 | 58.5 | 40.5 |
| | core | 1.2 | 59.3 | 39.5 |
| | core | 0.8 | 56.5 | 42.7 |
| | rim | 1.0 | 57.7 | 41.3 |
| | core | 1.1 | 60.2 | 38.6 |
| | rim | 1.5 | 59.0 | 39.6 |
| Tshirege Member: Sample No. | | | | |
| 77.04271.1 | | | | |
| (basal unwelded zone, cooling unit one) | core | 0.9 | 58.7 | 40.4 |
| | rim | 1.0 | 58.2 | 40.7 |
| | core | 0.9 | 55.9 | 43.3 |
| | rim | 0.8 | 58.9 | 40.3 |
| | core | 1.1 | 50.1 | 48.7 |
| | rim | 1.0 | 58.2 | 40.8 |
| 77.04274.1 | | | | |
| (zone of partial welding, cooling unit one) | core | 0.9 | 58.0 | 41.1 |
| | rim | 1.1 | 59.3 | 39.6 |
| | core | 0.9 | 59.2 | 39.9 |
| | rim | 0.9 | 57.2 | 41.9 |
| | core | 0.8 | 58.4 | 40.8 |
| | core | 1.1 | 58.0 | 40.9 |
| 77.04281.1 | | | | |
| (upper unwelded zone cooling unit one) | core | 1.0 | 58.0 | 40.2 |
| | rim | 1.2 | 59.8 | 38.9 |
| | overgrowth | 0.7 | 58.4 | 40.9 |
| | core | 1.4 | 59.0 | 39.6 |
| | rim | 1.7 | 59.6 | 38.7 |
| | core | 2.7 | 64.1 | 33.2 |
| | rim | 1.6 | 60.5 | 37.8 |

APPENDIX IV: Alkali Feldspar Compositions, Otowi and Tshirege Members.

Otowi Member: Sample No.

| | | An | Ab | Or |
|---|---|---|---|---|
| 77.4216.2 | | | | |
| | core | 1.2 | 55.3 | 43.5 |
| | rim | 2.3 | 61.4 | 36.3 |
| | core | 1.9 | 57.7 | 40.4 |
| | rim | 2.2 | 58.2 | 39.6 |
| | core | 1.5 | 56.4 | 42.1 |
| | rim | 1.6 | 57.7 | 40.7 |
| 77.04220.2 | | | | |
| | core | 1.4 | 55.9 | 42.7 |
| | rim | 1.2 | 56.8 | 42.0 |
| | core | 1.3 | 56.0 | 42.7 |
| | rim | 1.5 | 59.2 | 39.3 |
| | core | 1.3 | 59.2 | 39.5 |
| | rim | 1.64 | 57.1 | 41.3 |
| 77.04228.2 | | | | |
| | core | 2.1 | 57.9 | 40.0 |
| | core | 1.8 | 57.9 | 40.3 |
| | rim | 2.2 | 60.0 | 37.9 |
| | core | 1.34 | 56.6 | 42.0 |
| | rim | 1.45 | 56.7 | 41.8 |
| 77.04232.2 | | | | |
| | core | 1.3 | 58.6 | 40.1 |
| | rim | 1.6 | 59.5 | 38.9 |
| | core | 1.6 | 59.2 | 39.3 |
| | rim | 1.9 | 61.6 | 36.5 |
| | core | 1.4 | 57.8 | 40.8 |
| | rim | 2.0 | 62.4 | 35.6 |
| | core | 1.8 | 59.4 | 38.8 |

APPENDIX IV (Cont'd.)

| | | | | |
|---|---|---|---|---|
| 77.04289.1 | | | | |
| (zone of partial welding, cooling unit two) | core | 1.3 | 58.9 | 41.8 |
| | rim | 1.8 | 58.6 | 39.6 |
| | core | 1.3 | 58.5 | 40.2 |
| | rim | 1.4 | 58.3 | 40.4 |
| | core | 1.3 | 59.2 | 39.5 |
| | rim | 1.4 | 59.5 | 39.0 |
| 77.04290.1 | (Base, welded zone - unit 2) | | | |
| (zone of partial welding, cooling unit two) | core | 1.2 | 56.5 | 42.3 |
| | core | 1.2 | 56.7 | 42.1 |
| | rim | 1.1 | 57.7 | 41.2 |
| | core | 1.7 | 59.0 | 39.2 |
| | rim | 1.9 | 64.0 | 34.1 |
| | core | 1.3 | 58.0 | 40.8 |
| 77.04305.1 | | | | |
| (zone of partial welding, cooling unit three) | core | 1.7 | 58.3 | 39.9 |
| | rim | 1.42 | 58.6 | 40.0 |
| | overgrowth | 0.7 | 56.7 | 42.6 |
| | core | 1.7 | 58.4 | 39.9 |
| | rim | 1.5 | 56.7 | 41.8 |
| | core | 3.1 | 63.5 | 33.5 |
| 77.04306.2 | | | | |
| (upper unwelded zone, cooling unit three) | core | 1.4 | 57.5 | 41.2 |
| | core | 4.0 | 63.3 | 32.7 |
| | rim | 4.4 | 69.3 | 26.3 |
| | core | 2.0 | 58.3 | 39.8 |
| | rim | 2.9 | 62.2 | 34.9 |
| | core | 3.7 | 62.8 | 33.5 |

☆ U.S. GOVERNMENT PRINTING OFFICE: 1978—777-089/66